GENERAL ATOMIC

GA-A13923
UC-77

PREIRRADIATION REPORT OF TRISO AND BISO COATED ThO_2 PARTICLES FOR IRRADIATION IN CAPSULES HT-31 AND HT-33

by
W. J. KOVACS, C. A. YOUNG
and D. P. HARMON

Prepared under
Contract E(04-3)-167
Project Agreement No. 17
for the San Francisco Operations Office
U.S. Energy Research and Development Administration

GENERAL ATOMIC PROJECT 3224 DATE PUBLISHED: NOVEMBER 1976

ABSTRACT

The HT-31 and HT-33 irradiation capsules are part of a continued cooperative effort between General Atomic and Oak Ridge National Laboratory designed to evaluate irradiation performance of unbonded TRISO and BISO coated ThO_2 particles. Sixteen TRISO samples will be tested in HT-31 and thirty two TRISO and BISO samples will be irradiated in HT-33. The fuel will be tested at either 1200° or 1500°C to a fast fluence of 5 to 10 x 10^{25} n/m^2 $(E > 29\ fJ)_{HTGR}$. The evaluation tests will consist mainly of particles fabricated in the GA pilot plant 240-mm-diameter coater. The experimental test matrix for the TRISO and BISO particles is directed toward defining relationships between the outer pyrocarbon coating density, anisotropy, and coating rate and fuel particle performance. Detailed discussions of the TRISO and BISO particles being tested are presented in separate sections of the report.

CONTENTS

FIGURES

FIGURES (continued)

TABLES

TABLES (Continued)

1. INTRODUCTION

The HT-31 and HT-33 irradiation capsules are part of a continued cooperative effort between General Atomic (GA) and Oak Ridge National Laboratory (ORNL) and are funded by the ERDA-sponsored HTGR Fuels and Core Development Program. Specifically, these two capsules are designed to characterize the irradiation behavior of unbonded BISO and TRISO coated ThO_2 fertile fuel particles. The experiments are designated to be conducted in the target position of the High-Flux Isotope Reactor (HFIR) at ORNL. The experimental design and operation are similar to the HT-12 through HT-15 and HT-17 through HT-19 series. Experiments of this type are conducted in the target position (HT) of the HFIR because the high fluxes in the reactor allow the accumulation of high fast neutron doses and high thorium burnups in a short time.

HFIR target (HT) experiments provide a rapid means of evaluating and screening fuel materials and material variables which are being considered for use in HTGRs. The materials being evaluated in capsules HT-31 and HT-33 are coatings which have been deposited in the GA pilot plant 240-mm-diameter freon-cooled coater. The coater design and coater charge sizes represent a significant change in process conditions in comparison with conditions used to fabricate previous irradiation capsule samples. The experimental test matrix for unbonded TRISO and BISO coated particles is directed toward defining relationships between outer pyrocarbon coating (OPyC) density, anisotropy, and coating rate and fuel particle performance. It is considered necessary to test particles fabricated in the large coater prior to committing material to the final series of qualification tests.

This report presents the preirradiation evaluation of fuel particles tested in capsules HT-31 and HT-33. A description of the capsules is given in Section 2. Section 3 is devoted exclusively to TRISO coated ThO_2 particles tested in capsules HT-31 and HT-33. Section 4 is devoted to BISO coated ThO_2 particles tested in capsule HT-33.

2. CAPSULE DESCRIPTION

Capsules HT-31 and HT-33 will be irradiated in the target region (HT) of the HFIR at ORNL. Each capsule will contain four tubular graphite specimen holders or magazines located vertically in an aluminum tube. Each magazine will house 13 small graphite crucibles which hold the unbonded coated particles in annular cavities. Eight of the 13 graphite crucibles will be used for fertile particle samples. The other crucibles will contain low enriched UO_2 particles to produce a more uniform power generation and temperature over the life of the experiment. After the four magazines are loaded, each capsule will be sealed with 99.995% pure Ar at a pressure of 0.14 MPa (5 psig) and therefore no in-pile fission gas release can be measured. Since the capsules are uninstrumented, no temperatures will be measured during the irradiation. The operating temperatures will be estimated by ORNL based on the thermal analysis.

Capsule HT-31 began irradiation on March 14, 1976 and was discharged in June after four irradiation cycles. Capsule HT-33 is scheduled to be inserted in the reactor on June 17, 1976 and to be removed in October 1976; this capsule is designated for five irradiation cycles.

3. TRISO COATED ThO_2 PARTICLES

W. J. Kovacs

3.1. OBJECTIVES

The objectives for the testing of TRISO coated ThO_2 particles in capsules HT-31 and HT-33 are, in decreasing order of priority, as follows:

1. Evaluate the irradiation performance of unbonded TRISO coated ThO_2 particles fabricated in the 240-mm-diameter pilot plant coater and establish performance criteria equivalent to those for particles of similar designs and coating properties fabricated in the prototype 127-mm-diameter coater. Fabricating fuel particles in the large coater is part of the planned processing scale-up and verification of applicability of previous specifications to the scaled-up process is desirable. The samples will be irradiated at nominal temperatures of 1200° and 1500°C over an estimated fast neutron exposure $(E > 29\ fJ)_{HTGR}$ between 3.9 and 9.7 x 10^{25} n/m^2. Tables 3-1 and 3-2 give the design test conditions and a general description of fuel particle attributes. The exposure corresponds to an estimated fuel burnup between 4.5 and 12.5% FIMA.*

2. An equally important objective is to evaluate TRISO coated 450-μm-diameter ThO_2 particles as a potential backup design for BISO coated ThO_2 particles. The TRISO coated particle offers a design option which is expected to be more retentive of fission product release compared to BISO particles. In addition the new TRISO coated ThO_2 design represents an effort to reduce the performance risk associated with the old reference TRISO coated 500-μm-diameter ThO_2 particle. Empirical evidence indicates that there is a particle size effect governing performance, viz., the

*Fissions per initial metal atom.

probability of particle failure increases with particle size. Consequently, a comparative evaluation between 500-μm-diameter TRISO coated ThO_2 particles tested in capsules HT-28 and HT-29 and the HT-31 and HT-33 tests should serve to establish anticipated performance benefits in the TRISO coated 450-μm-diameter ThO_2 design. Capsules HT-31 and HT-33 will both include a sample from a batch of TRISO coated 500-μm-diameter ThO_2 particles (Batch 6252-05-0160) irradiated in capsules HT-28 and HT-29, which will provide a benchmark for comparing results.

3. A secondary set of objectives is to define empirical relationships between fuel performance and OPyC variables: density, anisotropy, coating rate, and oriented porosity. Figure 3-1 is a schematic diagram of the variable test matrix for TRISO coated fuel tested in capsules HT-31 and HT-33. Seven separate batches are grouped into two ranges of coating rates and a subgrouping of different bulk densities. A further subdivision (different coater bed sizes) exists for two sets of batches in order to characterize the degree of oriented porosity, which generally increases with the coater bed surface area.

3.2. TEST DESCRIPTION

Capsules HT-31 and HT-33 each contain a total of 32 different positions. The TRISO coated ThO_2 particles will occupy 16 positions in HT-31 and in HT-33. The unbonded particle locations in each capsule are divided into two sections: eight positions at 1500°C and eight positions at 1200°C. The design fast fluence for positions operating at 1200°C will be from 3.9 to 7.6 x 10^{25} n/m^2 $(E > 29\ fJ)_{HTGR}$ while positions at 1500°C will operate from 7.0 to 9.7 x 10^{25} n/m^2 $(E > 29\ fJ)_{HTGR}$.

Particle loadings were determined by defining design values for power densities through an appropriate thermal analysis and specifying the necessary thorium loadings to maintain the required temperatures in HT-31 and HT-33. Correspondingly, the total number of particles per position was determined by dividing the thorium weight per particle and the total allowable thorium weight for a designated position.

3.3. FUEL SAMPLE DESCRIPTION

The TRISO coated ThO_2 particles for irradiation in HT-31 and HT-33 were selected so that the particles within each individual sample had a constant total coated particle density and a narrow distribution of kernel and total coated particle diameters. The steps used to separate desired particles from their respective parent batches are outlined in Fig. 3-2. Briefly, coated particles were sieved to narrow the range in particle diameter. They were then further separated by selecting, via constant density liquid columns, only those particles having the batch-average total coated particle density. Following density separation, particles were individually radiographed to characterize each sample. Particles were subsequently heated in vacuum for 1 hr at 1400°C to ensure volatilization of any of the fluids used for density separation. As a final step, particles were heat treated for 0.5 hour at 1800°C in Ar; this step is taken to simulate the processing temperature that fuel particles would be exposed to during fuel rod fabrication. Preparing samples by these techniques also facilitates determining particle dimensional changes during the irradiation since their density and hence volume can easily be measured after irradiation.

Tables 1 and 2 show that the number of ThO_2 particles in different positions is limited to between 34 and 80 particles. Fuel failure within these limited groups of particles is adequate to establish qualitative "gross effects" between different coating attributes. A meaningful quantitative description of fuel failure fraction versus coating attribute is not possible because of the limited statistical size of the samples in each irradiation position; e.g., 330 particles have to be examined with no observed failures to have 95% confidence that the failure fraction in this group is less than 0.01. Thus, the HT-31 and HT-33 capsules are designed to serve as screening tests to determine success or failure between different particle groups and possibly focus on mechanisms contributing to particle failure. A subsequent test employing a larger group size of particles with similar attributes would then be

used to substantiate in a statistically relevant manner any predictions made from the HT-31 and HT-33 tests.

Figure 3-1 is a schematic diagram of the test matrix for the ThO_2 particles. The test matrix depicts a systematic variation for three independent variables, viz, OPyC coating rate and bulk density as primary variables with coater bed size being a secondary effect probably related to oriented porosity.

3.3.1. Selective Particle Segregation

Loose particles tested in capsules HT-31 and HT-33 were screened and density separated from the parent batch. Selective particle separation offers a convenient method for reducing the standard deviation about the mean for several particle variables; a quantitative description of kernel and coating layer variability within a particle is given in Ref. 3-1. Consequently, the confidence in test results is improved when relating total particle or coating layer performance to a given range of particular variables. Tables 3-1 through 3-5 give a summary description of TRISO coated particle attributes for samples irradiated in capsules HT-31 and HT-33. Photomicrographs of particles from each of the density-separated batches are shown in Figs. 3-3 through 3-10.

3.3.2. Coating Characterization

3.3.2.1. Pyrocarbon Characterization

Density and optical anisotropy are two principal parameters used to characterize the structure and irradiation stability of pyrocarbons. These parameters are listed in Tables 3-4 and 3-5 for the parent batches of TRISO coated particles tested in HT-31 and HT-33. Table 3-4 lists both OPTAF* and BAF_o* for the IPyC and OPyC coating layers. BAF_o is determined

*Acroynms signifying a crystallite anisotropy factor determined optically by intensity measurements of reflected polarized light which is rotated 360° about the pyrocarbon substrate.

by measuring without an analyzer (Seibersdorf unit) the ratio of reflected intensity parallel and perpendicular to the pyrocarbon substrate and calculating by an empirical equation the equivalent BAF determined by x-ray measurements. In contrast OPTAF is determined as the ratio of the maximum to minimum intensity of reflected light with the analyzer in the crossed position (General Atomic Quality Control unit). Both BAF_o and OPTAF are listed to provide a comparative data base for judging the sensitivity of each parameter to irradiation performance, i.e., OPyC survival. BAF_o measurements on TRISO coated particles indicate that the degree of crystallite anisotropy in IPyC layers ($1.065 \leq BAF_o \leq 1.098$) is greater than anisotropy in OPyC layers ($1.018 \leq BAF_o \leq 1.036$). Initial conjecture favored the viewpoint that the IPyC anisotropy increased over that of the as-deposited structure by exposure to coating temperatures (1550° to 1650°C) experienced during SiC deposition. This hypothesis was tested by measuring BAF_o at the BISO stage for specimens heat treated at different temperatures. The results are summarized as follows:

Thermal Treatment	BAF_o
As-coated through IPyC stage	1.051
1 hour at 1550°C	1.088
2 hours at 1550°C	1.086
3 hours at 1550°C	1.082
3 hours at 1550°C + 1/2 hour at 1650°C	1.087
1/2 hour at 1850°C	1.112

The results indicate that optical anisotropy of the as-coated IPyC layer is altered by thermal treatments between 1550° and 1650°C, i.e., temperatures and times comparable to maximum conditions expected during SiC deposition. At 1550°C the BAF_o increase (1.051 to 1.088) occurs in less than 1 hour, and is subsequently insensitive to time in the temperature range 1550° to 1650°C. However, a 0.5-hour heat treatment at 1850°C resulted in a further BAF_o increase to 1.112. The increase in optical anisotropy is attributed to pyrocarbon densification, crystallite realignment, or a combination of both effects. Tentatively, it is concluded that the high IPyC BAF_o is a result of temperatures experienced during SiC deposition.

Previous irradiation experience indicates that high IPyC failure fractions are probable for HT-31 and HT-33 particles, based on BAF_o mean values ≥ 1.065. This should not adversely affect the performance of TRISO coated particles in that the IPyC phase is designed as an impervious layer to prevent kernel contamination by volatile species (Cl) produced during SiC deposition. A fraction of the batch of large-diameter TRISO coated particles (>830 μm) experiences failure of the OPyC phase at a batch mean $BAF_o \gtrsim 1.023$ (Ref. 3-2). The tablulated batch mean BAF_o values in Table 3-4 range between 1.022 and 1.034; consequently, limited OPyC failure is predicted on particles tested in capsules HT-31 and HT-33 at the highest exposure condition.

Bulk densities of the IPyC phase (ρ_I) in parent batches are listed in Table 3-5 and are bounded by $1.71 \leq \rho_I \leq 1.79$ Mg/m^3. This density range provides a limit to Hg intrusion at ∿68.9 MPa (10 ksi), and it is inferred that the IPyC structure should be impermeable to large gaseous species (no interconnecting porosity greater than 100 Å in extent). Bulk OPyC densities (ρ_0) were selectively fabricated to $1.55 \leq \rho_0 \leq 1.81$ Mg/m^3, sufficient to evaluate performance and to define acceptable fuel specification limits.

The accessible porosity in the IPyC and OPyC layers was measured by Hg instrusion at ∿68.9 MPa (10 ksi) (listed in Table 3-5). Accessible porosity was between 40.5 and 62 μℓ/g PyC coating, and there does not appear to be a correlation with the coater batch size. However, a comparative metallographic evaluation of the pore structure in OPyC layers (shown in Fig. 3-11) depicts two representative types: (1) laminated or oriented porosity associated with a coater charge size of 10 to 13 kg of Th at the OPyC stage, and (2) dispersed porosity associated with a coater charge size of 4.6 to 6.6 kg of Th at the OPyC stage. The paired batches in this figure have essentially equivalent bulk densities and optical anisotropies; consequently, the effect of pore structure on OPyC survival should be considered in evaluating performance if differences in performance are observed.

3.3.2.2. SiC Characterization

TRISO coated batches produced in the 240-mm-diameter coater (designs 6252-06 through 6252-10) originated from two SiC parent batches. Microstructural evaluation of the SiC phase in both of these batches indicated the presence of voids in a large fraction of the SiC layers, characterized by a distribution of flaw sizes up to a maximum of 500 μm. Flaw morphology in the SiC phase is characterized as having equal dimensions in the circumferential direction with an aspect ratio (circumferential-to-radial flaw size) of ∿10.

Figure 3-12 shows a range of flaw sizes in a diametral cross section. The translucent property of thin sections of SiC allows the detection of internal reflecting surfaces within the layer. Optical evaluation (∿30X) of all batches burned back to the SiC phase showed that approximately 24% of the particle population had localized discolorations, i.e., a golden or white hue, present in the SiC layers. These discolorations were attributed to reflections from internal SiC flaw surfaces and were distinctive against a uniform shiny grey background (the reflection of the IPyC layers through the SiC). A one-to-one correspondence between the optically and metallographically observed defects in the SiC phase is further supported by the observed frequency of defects in two- and three-dimensional sections.

The correspondence between optical discolorations in the SiC phase and internal flaws offers a convenient method for defining the flaw size distribution; i.e., equate flaw size to extent of optical discoloration. Figure 3-13 is a frequency distribution of the flaw size present in defective SiC layers. This distribution was used to calculate a SiC fracture strength distribution by assuming:

1. A uniform applied tensile stress across SiC phase.
2. Brittle fracture described by the Griffith-Orowan relation.

The SiC fracture strength, σ_F, is defined as

$$\sigma_F = k\left(\frac{E \cdot \gamma_f}{C}\right)^{1/2} \quad , \tag{3-1}$$

where k is a geometric factor related to the crack morphology, i.e., lenticular flaws, which can be considered proportional to a stress intensity factor (assumed $\sim$1). E is the elastic modulus, γ_f is the fracture surface energy, and C is the flaw length (defined perpendicular to the applied tensile stress). Recently, Coppola (Ref. 3-3) measured γ_f and E for a number of polycrystalline SiC specimens; values which most closely relate to vapor-deposited SiC structures are taken as $\gamma_f^* = 28.7 \times 10^3$ ergs/cm^2 and E = 3.72×10^{12} dynes/cm^2. The maximum flaw size is in the circumferential direction and parallel to the applied tensile stress resulting from internal pressure in the TRISO particle. The aspect ratio of flaw sizes (circumferential:radial) as depicted in Fig. 3-12 is $\sim$10 and is assumed independent of flaw size. This provides the basis for defining the critical flaw dimension perpendicular to the applied tensile stress, i.e., chosen as $\sim$0.1 of the maximum optical flaw size. Equation 3-1 was used to calculate the fracture strengths for different optically observed flaw sizes. The calculated fracture strength distribution, shown in Fig. 3-14, is skewed to the right with a median fracture strength of $\sim$55 MPa (7.98 ksi); i.e., 50% of the defective SiC layers have a fracture strength between 20 and 55 MPa (2.90 to 7.98 ksi). Defective SiC layers (fracture strengths below a critical value) will result in premature pressure vessel failure in a test population; the effect is predictable if the particle stress distribution, $P(\sigma)$, is determined:

$$\hat{f}_s = \int_o^\infty P(\sigma)\left[\int_o^\sigma F(\sigma_F)\, d\sigma\right] d\sigma \quad , \tag{3-2}$$

---

*γ_f is considerably higher than the intrinsic surface energy of covalently bonded materials. The measured value is best termed an "effective work of fracture" and reflects a rough intergranular fracture mode.

where $\hat{f}_s$ = anticipated mean failure fraction,

$P(\sigma)$ = frequency of maximum tangential stress, σ, in TRISO particle population,

$F(\sigma_F)$ = frequency of SiC fracture strength, σ_F, in TRISO particle population.

Figure 3-15 is a schematic diagram illustrating arbitrary particle stress and fracture strength distributions superimposed on the same coordinates. The distribution of coating stresses, $P(\sigma)$, for a given test population can be determined by a Monte Carlo calculational method which accounts for the variability of different particle phases, viz, the influence of kernel, buffer IPyC, and SiC thicknesses and densities on the maximum tangential stress in the SiC layer. The particle stress is based on a thick-walled elastic sphere with fission gas production causing a progressive increase in the internal pressure and maximum tensile stress in the SiC layer of any particle.

Anisotropic dimensional changes resulting in densification of the OPyC phase cause residual compressive stresses approximating 103 MPa (15 ksi) to develop in the pyrocarbon for fast fluence exposures between 2.5 and 8.0 x 10^{25} n/m^2 $(E \geq 29\ fJ)_{HTGR}$ (Ref. 3-4). The compressive stress reduces the maximum tensile stress buildup in the SiC layer. Calculations for the particle stress distribution, $P(\sigma)$, in a TRISO coated population assume that a constant compressive stress of 103 MPa (15 ksi) is exerted by the OPyC phase on each particle. This is an approximate assumption in that variability in the compressive stress in this phase exists across the entire OPyC population. Explicit functions to describe the dependence of optical anisotropy, density, and thickness in OPyC layers on compressive stress are not well defined and consequently an assumed constancy of stress is a reasonable first approximation. This approach was used to calculate $P(\sigma)$ and a corresponding failure fraction $\hat{f}_s$ for representative test populations in capsule HT-31. Batches 6252-06-010 to 6252-08-010 inclusive all have the same generic origin through the SiC phase and should exhibit comparable $P(\sigma)$ and $F(\sigma_F)$ distributions. Exposure conditions vary for different test populations in HT-31; however, Table 3-6 lists the expected range of failure fractions for two extreme test conditions. The predicted

range of TRISO particle failure under these assumptions is:

$$0.02\% \leq \hat{f}_s \leq 12\% \quad .$$

Confirmation of the anticipated failure fracture would imply the failure probability in TRISO coated ThO_2 can be correlated with SiC flaw size.

A further refinement can be made during the PIE of capsules HT-31 and HT-33 by correlating the observed failure fractions with $F(\sigma_F)$ through Eq. 3-2, effectively normalizing the SiC fracture strength distribution against test results. The normalized distribution of $F(\sigma_F)$ could then be used as a basis for performance predictions in future test populations of TRISO coated ThO_2.

REFERENCES

3-1. Kovacs, W. T., and D. P. Harmon, "Preirradiation Report, HT-28 and HT-29," ERDA Report GA-A13276, General Atomic Company, June 13, 1975, p. 8.

3-2. Harmon, D. P., and C. B. Scott, "Development and Irradiation Performance of LHTGR Fuel," ERDA Report GA-A13173, General Atomic Company, October 31, 1975, pp. 85 to 95.

3-3. Coppola, J. A., and R. C. Bradt, J. Am. Ceram. Soc. 55, 455 (1972).

3-4. Gulden, T. D., et al., Nucl. Technol. 16, 100 (1972).

TABLE 3-1
GENERAL DESCRIPTION OF TRISO COATED PARTICLES TESTED IN CAPSULE HT-31

Particle Batch Data Retrieval Number	Kernel Mean Diameter (μm)	Coating Phases												Total Coated Particle						Test Conditions					
		Buffer		IPyC				SiC		OPyC															
		Thickness (μm)	Density[a] (Mg/m^3)	Thickness (μm)	Density[a] (Mg/m^3)	Coating Rate (μm/min)	BAF_o[b]	Thickness (μm)	Density[a] (Mg/m^3)	Thickness (μm)	Density[a] (Mg/m^3)	Coating Rate (μm/min)	BAF_o[b]	Coating Thickness (μm)	Mean Diameter (μm)	Mean Density[c] (Mg/m^3)	Th-232 Particle Loading[d] (μg/particle)	Exposed Heavy Metal[e] ($\frac{\mu g \text{ heavy metal}}{g \text{ heavy metal}}$)	Defective SiC Fraction[f] ($\frac{\mu g \text{ Th leached}}{\text{total g Th}}$)	X-ray Plate I.D.	Number of Particles Tested	Sample Position	Design Test Temperature (°C)	Design Peak Fast Fluence ($E > 29$ fJ) HTGR (10^{25} n/m^2)	Design Burnup (% FIMA)
6252-05-0160-005	511	69	1.04	30	1.84	3.93	ND[g]	35	3.20	48	1.85	4.40	ND	176	873	3.59	654	2	36	LB341	34	43	1200	5.6	6.2
6252-05-0160-006	509	68	1.04	30	1.84	3.93	ND	34	3.20	50	1.85	4.58	ND	176	872	3.59	654	2	36	LB342	51	27	1500	7.7	8.4
6252-06-0161-001	449	69	1.07	34	1.90	4.09	1.076	41	3.22	45	1.74	5.00	1.022	181	819	3.39	429	8.3	2.7	LB346	53	49	1200	4.4	5.0
6252-06-0161-002	448	68	1.07	34	1.90	4.09	1.076	41	3.22	44	1.74	4.89	1.022	181	823	3.39	429	8.3	2.7	LB347	78	38	1500	7.0	7.7
6252-06-0261-001	448	60	1.12	39	1.93	4.43	1.088	39	3.21	47	1.70	5.34	1.028	190	813	3.26	424	0.8	120	LB361	52	48	1200	4.7	5.2
6252-06-0261-002	448	59	1.12	39	1.93	4.43	1.088	39	3.21	46	1.70	5.23	1.028	190	812	3.26	424	0.8	120	LB362	77	36	1500	7.3	7.9
6252-07-0161-001	448	57	1.12	39	1.93	4.43	1.079	39	3.20	50	1.81	5.56	1.027	191	816	3.23	415	9.2	10.6	LB366	54	46	1200	5.0	5.6
6252-07-0161-002	448	58	1.12	39	1.93	4.43	1.079	40	3.20	52	1.81	5.78	1.027	191	823	3.23	415	9.2	10.6	LB367	80	35	1500	7.4	8.0
6252-07-0261-001	447	63	1.12	39	1.93	4.43	1.098	39	3.21	46	1.80	5.11	1.030	187	820	3.32	423	0.8	3.5	LB371	53	45	1200	5.2	5.8
6252-07-0261-002	446	62	1.12	39	1.93	4.43	1.098	39	3.21	47	1.80	5.22	1.030	187	821	3.32	423	0.8	3.5	LB372	78	33	1500	7.5	8.2
6252-08-0161-001	447	60	1.12	39	1.93	4.43	1.065	39	3.20	49	1.89	5.44	1.034	194	836	3.30	414	1	18	LB336	54	51	1200	3.9	4.5
6252-08-0161-002	447	60	1.12	39	1.93	4.43	1.065	39	3.20	50	1.89	5.56	1.034	194	836	3.30	414	1	18	LB337	80	29	1500	7.7	8.4
6252-09-0161-001	447	66	1.07	34	1.90	4.09	1.095	41	3.22	47	1.78	7.23	1.018	185	823	3.34	426	1	7.2	LB356	53	42	1200	5.9	6.4
6252-09-0161-002	447	63	1.07	34	1.90	4.09	1.095	42	3.22	48	1.78	7.38	1.018	185	819	3.34	426	1	7.2	LB357	78	32	1500	7.6	8.2
6252-10-0161-001	447	63	1.07	34	1.90	4.09	1.074	42	3.22	53	1.98	8.15	1.036	189	829	3.31	421	2	8.4	LB351	53	40	1200	6.2	6.8
6252-10-0161-002	446	62	1.07	34	1.90	4.09	1.074	42	3.22	51	1.98	7.85	1.036	189	824	3.31	421	2	8.4	LB352	79	30	1500	7.6	8.3

[a] Measured on parent batch prior to density separation.

[b] Measured on nonheat-treated parent batch. Bacon Anisotropy Factor determined optically using 24-μm-diameter spot.

[c] Determined by Hg porosimeter.

[d] Calculated from density and thickness of parent batch coating phases and ThO_2 stoichiometry.

[e] Determined by hydrolysis test on parent batch and indicates total amount of exposed heavy metal; not corrected for partial conversion of oxide to carbide.

[f] Determined by burn and 24-hr ultraleach on parent batch.

[g] ND = not determined.

TABLE 3-2
GENERAL DESCRIPTION OF TRISO COATED PARTICLES TESTED IN CAPSULE HT-33

Particle Batch Data Retrieval Number	Kernel Mean Diameter (μm)	Coating Phases												Total Coated Particle						Test Conditions					
		Buffer		IPyC				SiC		OPyC															
		Thickness (μm)	Density[a] (Mg/m^3)	Thickness (μm)	Density[a] (Mg/m^3)	Coating Rate (μm/min)	BAF_o[b]	Thickness (μm)	Density[a] (Mg/m^3)	Thickness (μm)	Density[a] (Mg/m^3)	Coating Rate (μm/min)	BAF_o[b]	Coating Thickness (μm)	Mean Diameter (μm)	Mean Density[c] (Mg/m^3)	Th-232 Particle Loading[d] (μg/particle)	Exposed Heavy Metal[e] (μg heavy metal / g heavy metal)	Defective SiC Fraction[f] (μg Th leached / total g Th)	X-ray Plate I.D.	Number Of Particles Tested	Sample Position	Design Test Temperature (°C)	Design Peak Fast Fluence ($(E > 29\ fJ)_{HTGR}$ $(10^{25}\ n/m^2)$)	Design Burnup (% FIMA)
6252-05-0160-007	509	68	1.04	30	1.84	3.93	ND[g]	35	3.20	50	1.85	4.58	ND	176	872	3.59	654	2	36	LB343	34	45	1200	6.5	9.4
6252-05-0160-008	510	68	1.04	30	1.84	3.93	ND	34	3.20	48	1.85	4.40	ND	176	870	3.59	654	2	36	LB344	51	30	1500	9.6	12.4
6252-06-0161-003	448	64	1.07	34	1.90	4.09	1.076	41	3.22	44	1.74	4.89	1.022	181	818	3.39	429	8.3	2.7	LB348	53	48	1200	5.9	8.0
6252-06-0161-004	450	68	1.07	34	1.90	4.09	1.076	41	3.22	46	1.74	5.11	1.022	181	824	3.39	429	8.3	2.7	LB349	78	33	1500	9.3	12.1
6252-06-0261-003	448	60	1.12	39	1.93	4.43	1.088	38	3.21	47	1.70	5.34	1.028	190	812	3.26	424	0.8	120	LB363	52	46	1200	6.3	8.6
6252-06-0261-004	449	59	1.12	39	1.93	4.43	1.088	39	3.21	48	1.70	5.45	1.028	190	816	3.26	424	0.8	120	LB364	77	32	1500	9.5	12.2
6252-07-0161-003	446	58	1.12	39	1.93	4.43	1.079	39	3.20	51	1.81	5.67	1.027	191	826	3.23	415	9.2	10.6	LB368	54	43	1200	6.9	9.5
6252-07-0161-004	447	58	1.12	39	1.93	4.43	1.079	38	3.20	52	1.81	5.78	1.027	191	821	3.23	415	9.2	10.6	LB369	80	36	1500	9.1	11.8
6252-07-0261-003	446	61	1.12	39	1.93	4.43	1.098	39	3.21	46	1.80	5.11	1.030	187	813	3.32	423	0.8	3.5	LB373	53	42	1200	7.3	9.7
6252-07-0261-004	447	62	1.12	39	1.93	4.43	1.098	38	3.21	46	1.80	5.11	1.030	187	814	3.32	423	0.8	3.5	LB374	78	35	1500	9.2	11.9
6252-08-0161-003	447	61	1.12	39	1.93	4.43	1.065	38	3.20	47	1.89	5.22	1.034	194	836	3.30	414	1	18	LB338	54	49	1200	5.5	7.5
6252-08-0161-004	448	61	1.12	39	1.93	4.43	1.065	38	3.20	50	1.89	5.56	1.034	194	836	3.30	414	1	18	LB339	80	27	1500	9.6	12.5
6252-09-0161-003	448	65	1.07	34	1.90	4.09	1.095	42	3.22	47	1.78	7.23	1.018	185	824	3.34	426	1	7.2	LB358	53	40	1200	7.6	10.2
6252-09-0161-004	447	67	1.07	34	1.90	4.09	1.095	42	3.22	49	1.78	7.54	1.018	185	826	3.34	426	1	7.2	LB359	78	38	1500	8.7	11.5
6252-10-0161-003	447	63	1.07	34	1.90	4.09	1.074	42	3.22	51	1.98	7.85	1.036	189	826	3.31	421	2	8.4	LB353	53	51	1200	4.9	7.0
6252-10-0161-004	445	62	1.07	34	1.90	4.09	1.074	42	3.22	51	1.98	7.85	1.036	189	818	3.31	421	2	8.4	LB354	79	29	1500	9.6	12.5

[a] Measured on parent batch prior to density separation.

[b] Measured on nonheat-treated parent batch. Bacon Anisotropy Factor determined optically using 24-μm-diameter spot.

[c] Determined by Hg porosimeter.

[d] Calculated from density and thickness of parent batch coating phases and ThO_2 stoichiometry.

[e] Determined by hydrolysis test on parent batch and indicates total amount of exposed heavy metal; not corrected for partial conversion of oxide to carbide.

[f] Determined by burn and 24-hr ultraleach on parent batch.

[g] ND = not determined.

TABLE 3-3
KERNEL DIAMETER AND COATING THICKNESS MEASUREMENTS ON TRISO COATED ThO_2 PARTICLES TESTED IN CAPSULES HT-31 AND HT-33

Particle Batch Data Retrieval Numbers		Kernel[a] Diameter (μm)		Buffer Thickness (μm)		IPyC Thickness (μm)		SiC Thickness (μm)		OPyC Thickness (μm)	
Parent Batch	Density Separated Batch	Mean	Standard Deviation	Calculated[b]	Standard Deviation	Mean[c]	Standard Deviation[c]	Mean	Standard Deviation	Mean	Standard Deviation
6252-05-015	6252-05-0160-005	511	5.81	69	6.72	30	5.10	35	2.65	48	4.44
	6252-05-0160-006	509	7.30	68	6.75	30	5.10	34	3.00	50	5.67
	6252-05-0160-007	509	5.50	68	5.97	30	5.10	35	2.97	50	5.17
	6252-05-0160-008	510	6.81	68	7.29	30	5.10	34	2.91	48	4.53
6252-06-010	6252-06-0161-001	449	5.43	69	7.68	34	4.70	41	2.87	45	5.76
	6252-06-0161-002	448	5.67	68	7.50	34	4.70	41	3.24	44	5.49
	6252-06-0161-003	448	4.72	64	7.52	34	4.70	41	2.53	44	6.42
	6252-06-0161-004	450	8.97	68	7.52	34	4.70	41	3.03	46	6.29
6252-06-020	6252-06-0261-001	448	6.54	60	7.41	39	4.78	39	2.80	47	5.61
	6252-06-0261-002	448	5.81	59	6.47	39	4.78	39	3.17	46	6.13
	6252-06-0261-003	448	5.27	60	7.52	39	4.78	38	3.05	47	5.90
	6252-06-0261-004	449	5.47	59	6.65	39	4.78	39	2.54	48	5.31
6252-07-010	6252-07-0161-001	448	6.62	57	6.67	39	4.78	39	2.09	50	6.66
	6252-07-0161-002	448	6.15	58	6.13	39	4.78	40	3.11	52	6.05
	6252-07-0161-003	448	5.68	58	6.42	39	4.78	39	2.72	51	7.05
	6252-07-0161-004	447	6.17	58	8.59	39	4.78	38	2.97	52	6.78
6252-07-020	6252-07-0261-001	447	5.53	63	5.98	39	4.78	39	3.38	46	5.81
	6252-07-0261-002	446	4.88	62	7.85	39	4.78	39	3.35	47	5.73
	6252-07-0261-003	446	4.54	61	6.55	39	4.78	39	3.23	46	6.68
	6252-07-0261-004	447	5.27	62	7.02	39	4.78	38	2.40	46	6.30
6252-08-010	6252-08-0161-001	447	4.50	60	7.73	39	4.78	39	2.75	49	6.68
	6252-08-0161-002	447	5.38	60	6.97	39	4.78	39	2.71	50	6.20
	6252-08-0161-003	447	5.52	61	7.24	39	4.78	38	3.12	47	6.24
	6252-08-0161-004	448	5.98	61	7.14	39	4.78	38	3.16	50	6.07
6252-09-010	6252-09-0161-001	447	4.43	66	7.62	34	4.70	41	2.78	47	5.66
	6252-09-0161-002	447	4.69	63	7.44	34	4.70	42	2.95	48	5.74
	6252-09-0161-003	448	5.27	65	7.03	34	4.70	42	3.37	47	5.00
	6252-09-0161-004	447	5.05	67	7.17	34	4.70	42	3.02	49	5.07
6252-10-010	6252-10-0161-001	447	6.40	63	7.90	34	4.70	42	2.83	54	6.55
	6252-10-0161-002	446	4.09	62	6.56	34	4.70	42	2.69	51	6.16
	6252-10-0161-003	447	5.43	63	6.93	34	4.70	42	3.54	51	5.16
	6252-10-0161-004	445	5.09	62	7.63	34	4.70	42	2.69	51	5.03

[a] The generic origin of all kernel batches is oxalate-derived ThO_2.

[b] Determined by subtracting the IPyC thickness from the measured buffer plus IPyC thickness.

[c] Dimensions measured on parent batch.

TABLE 3-4
COATING DENSITY, OPTICAL ANISOTROPY, AND COATING RATE MEASUREMENTS FOR TRISO COATED ThO_2 SAMPLES IN CAPSULE HT-31 AND HT-33 PARENT BATCHES

Particle Batch Data Retrieval Number	Coater Diameter (mm)	Coater Charge (kg Th at OPyC Stage)	IPyC[a]								SiC				OPyC[a]							
			Density (Mg/m^3)		Coating Rate (μm/min)		OPTAF[b]		BAF_o[b]		Density (Mg/m^3)		Coating Rate (μm/min)		Density (Mg/m^3)		Coating Rate (μm/min)		OPTAF		BAF_o[b]	
			Mean	Standard Deviation	Mean	Standard Deviation[c]	Mean	Standard Deviation	Mean	Standard Deviation	Mean	Standard Deviation	Mean	Standard Deviation[c]	Mean	Standard Deviation	Mean	Standard Deviation[c]	Mean	Standard Deviation	Mean	Standard Deviation
6252-05-015	127	0.7	1.84	8.45×10^{-3}	3.93	0.671	1.18	4.46×10^{-2}	ND[c]	ND	3.20	7.0×10^{-6}	0.254	2.07×10^{-2}	1.85	5.13×10^{-3}	4.48	0.467	1.12	3.99×10^{-2}	ND	ND
6252-06-010	241	10.20	1.90	2.32×10^{-2}	4.09	0.566	1.30	11.7×10^{-2}	1.076	8.8×10^{-3}	3.22	6.84×10^{-3}	0.225	2.458×10^{-2}	1.74	1.27×10^{-2}	5.04	0.754	1.11	4.83×10^{-2}	1.022	4.5×10^{-3}
6252-06-020	241	5.40	1.93	1.08×10^{-2}	4.43	0.543	1.30	9.51×10^{-2}	1.088	11.5×10^{-3}	3.21	3.59×10^{-3}	0.169	1.504×10^{-2}	1.70	1.09×10^{-2}	5.60	0.807	1.11	4.21×10^{-2}	1.028	4.1×10^{-3}
6252-07-010	241	13.20	1.93	1.08×10^{-2}	4.43	0.543	1.32	8.16×10^{-2}	1.079	7.1×10^{-3}	3.20	5.09×10^{-3}	0.168	1.20×10^{-2}	1.81	1.21×10^{-2}	5.92	0.778	1.15	6.16×10^{-2}	1.027	5.0×10^{-3}
6252-07-020	241	6.60	1.93	1.08×10^{-2}	4.43	0.543	1.31	9.87×10^{-2}	1.098	10.5×10^{-3}	3.21	3.93×10^{-3}	0.165	1.430×10^{-2}	1.80	2.45×10^{-2}	5.28	0.688	1.13	5.25×10^{-2}	1.030	3.0×10^{-3}
6252-08-010	241	10.80	1.93	1.08×10^{-2}	4.43	0.543	1.29	9.22×10^{-2}	1.065	3.6×10^{-3}	3.20	0	0.173	1.507×10^{-2}	1.89	1.08×10^{-2}	5.87	0.748	1.13	5.82×10^{-2}	1.034	6.2×10^{-3}
6252-09-010	241	10.50	1.90	2.32×10^{-2}	4.09	0.566	1.28	1.26×10^{-1}	1.095	13.9×10^{-3}	3.22	3.42×10^{-3}	0.223	1.869×10^{-2}	1.78	9.74×10^{-3}	7.52	0.814	1.11	4.56×10^{-3}	1.018	4.3×10^{-3}
6252-10-010	241	4.65	1.90	2.32×10^{-2}	4.09	0.566	1.24	6.42×10^{-2}	1.074	11.3×10^{-3}	3.22	3.36×10^{-3}	0.228	1.98×10^{-2}	1.98	0	8.43	0.971	1.14	5.10×10^{-2}	1.036	6.0×10^{-3}

[a] Vapor deposited coating from a mixed gas C_2H_2/C_3H_6 in a fluidized bed.

[b] Optical anisotropy and Bacon anisotropy factors are determined by optical intensity measurements of the polarization direction parallel and perpendicular to pyrocarbon substrate; BAF_o measured with 24-μm-diameter spot.

[c] Determined by assuming a constant coating time for each particle and applying standard deviation of thickness distribution.

[d] ND = not determined.

TABLE 3-5
PYROCARBON DENSITY AND POROSITY MEASUREMENTS FOR HT-31 AND HT-33 PARENT BATCHES

Particle Batch Data Retrieval Number	IPyC			OPyC			
				Density (Mg/m^3)			
	Measured Liquid Gradient Density (Mg/m^3)	Internal Porosity[a] ($\mu\ell$/g PyC)	Calculated Bulk Density[b] (Mg/m^3)	Measured Liquid Gradient	Measured Bulk[c]	Internal Porosity[a] ($\mu\ell$/g PyC)	Calculated Bulk Density[b] (Mg/m^3)
6252-05-015	1.84	ND[d]	ND	1.85	ND	ND	ND
6252-06-010	1.90	58.0	1.71	1.74	1.59	49[e]	1.60
6252-06-020	1.93	40.5	1.79	1.70	1.57	59[f]	1.55
6252-07-010	1.93	40.5	1.79	1.81	1.59	59[e]	1.63
6252-07-020	1.93	40.5	1.79	1.80	1.65	48[f]	1.66
6252-08-010	1.93	40.5	1.79	1.89	1.73	46[e]	1.74
6252-09-010	1.90	58.0	1.71	1.78	1.59	62[e]	1.60
6252-10-010	1.90	58.0	1.71	1.98	1.75	46[f]	1.81

[a] Internal porosity measured by Hg volume displacement at ~68.9 MPa.

[b] Calculated as $\rho_B = [\rho_S/(1 + \rho_S \cdot P)]$ where ρ_B = bulk density, ρ_S = liquid gradient density, and P = internal porosity/g PyC.

[c] Determined by measuring weight and Hg volume displacement at TRISO and burned-back particle stage.

[d] ND = not determined.

[e] Nominal coater charge size 10 to 13 kg Th at OPyC stage; refer to Table 3-4.

[f] Nominal coater charge size 4.6 to 6.6 kg Th at OPyC stage; refer to Table 3-4.

TABLE 3-6
MONTE-CARLO-BASED PARTICLE STRESS DENSITY DISTRIBUTIONS AND ESTIMATED FAILURE FRACTIONS FOR A TYPICAL POPULATION TESTED IN HT-31

Data Retrieval Number	Irradiation Conditions				Stress Density Distribution Parameters[a]			Percent of Population with Maximum Tensile Stresses at Least Greater Than Stresses Shown[a] (MPa)								Estimated Mean Failure Fraction[b]
	Cell Position	Temp (°C)	Fast Fluence ($E > 29$ fJ)$_{HTGR}$ (10^{25} n/m^2)	Burnup (% FIMA)	Mean (MPa)	Median (MPa)	Standard Deviation (MPa)	0	17.25	34.50	60	90	100	170	200	
6252-08-0161-001	51	1200	3.9	4.5	-27.6	-28.5	18.5	8.71	3.01	0.80	0.10	0	0	0	0	2×10^{-4}
6252-08-0161-001	29	1500	7.7	8.4	75.5	70.5	45.5	99.10	94.90	82.0	59.50	39.0	26.3	4.2	1.7	12×10^{-2}

[a] Particle stress distribution $P(\sigma)$; based on assumption of constant OPyC compressive stress of 103 MPa.

[b] Based on the convolution of the fracture strength $F(\sigma_F)$ and the particle stress $P(\sigma)$ distributions; refer to Eq. 3-2 and Fig. 3-15. $\hat{f}_s$ calculated from Eq. 3-2 was multiplied by 0.24 to account for that fraction of the SiC population which exhibited optical defects.

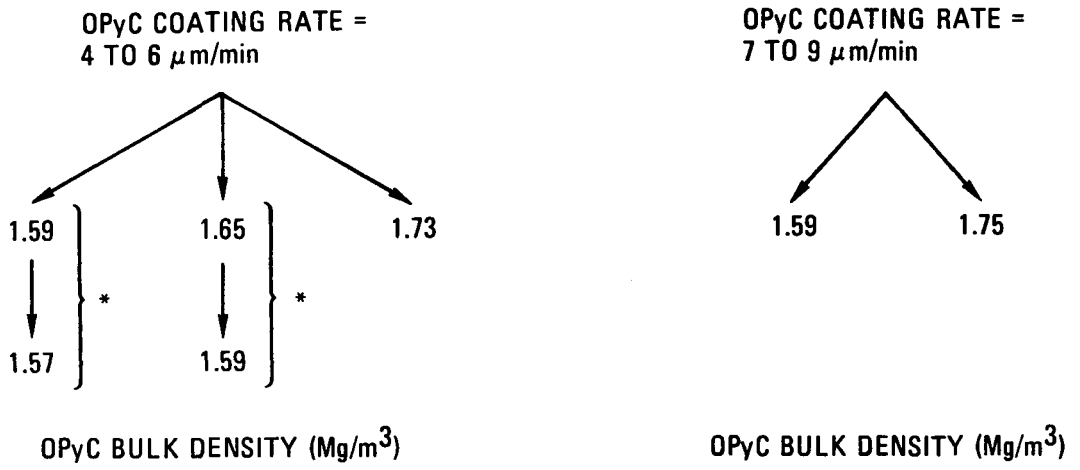

* DIFFERENCE BETWEEN BATCHES IN A SET IS THE INITIAL COATER BED SIZE; I.E., ONE BATCH WAS COATED WITH A Th CHARGE OF ~12 kg WHILE THE SECOND BATCH WAS COATED USING ~6 kg OF Th.

Fig. 3-1. Schematic diagram of test matrix for TRISO coated ThO_2 particles

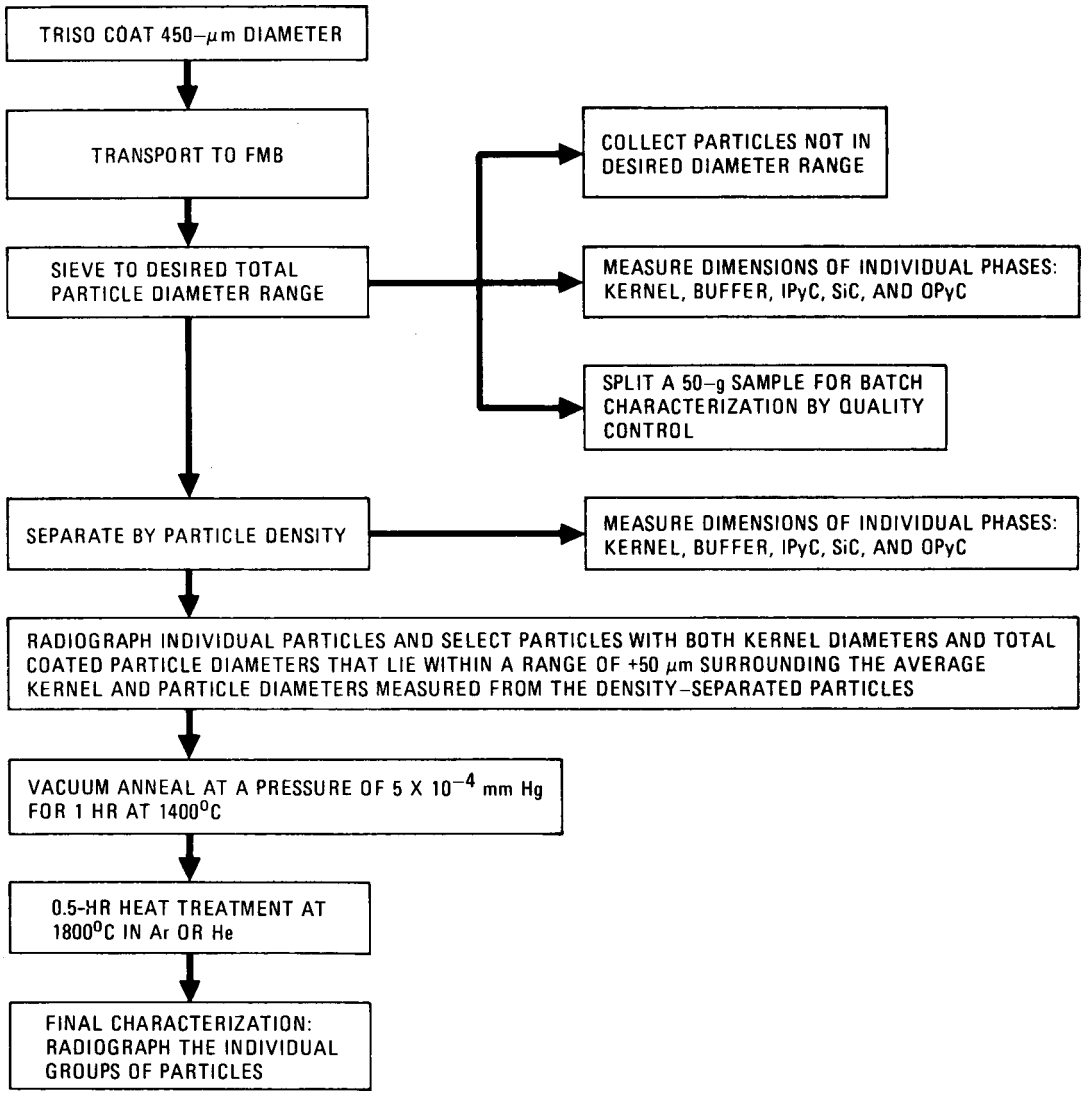

Fig. 3-2. Steps involved in selecting TRISO coated ThO_2 particles for insertion in irradiation experiments HT-31 and HT-33

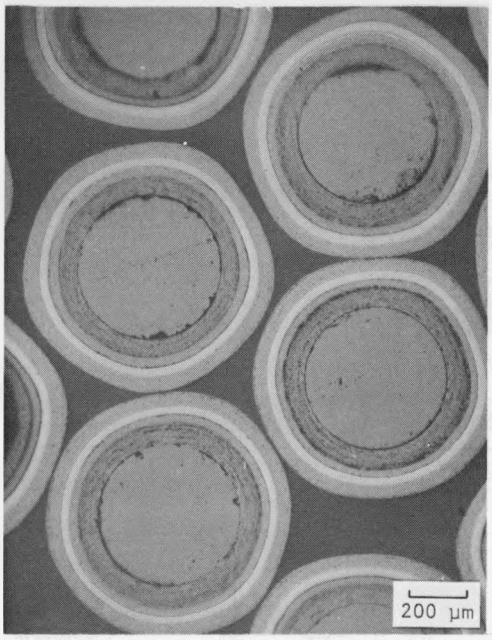

MP75019-6 (a)

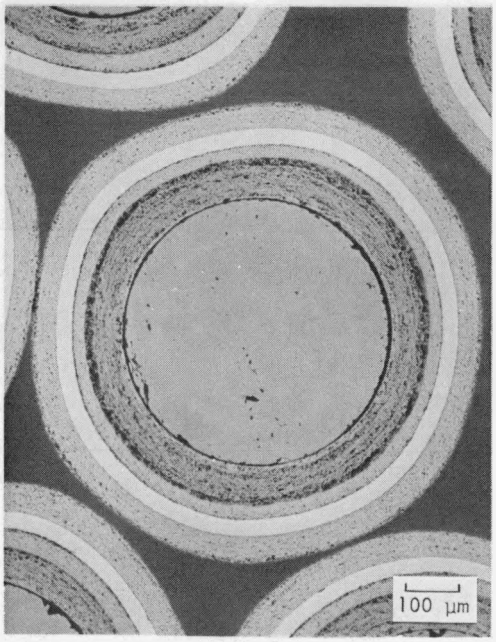

MP75019-1 (b)

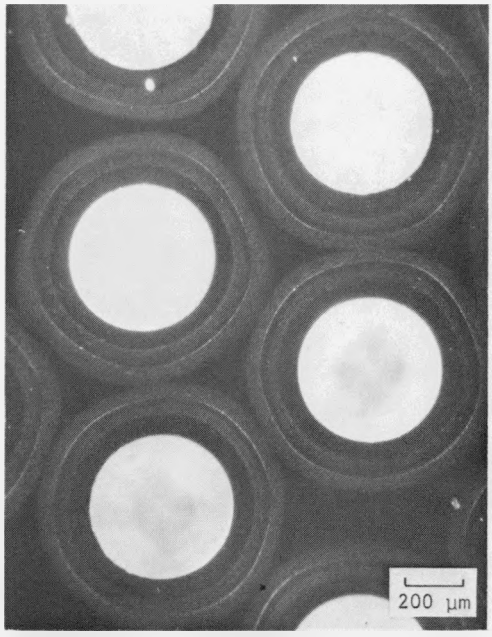

MP75019-7 (c)

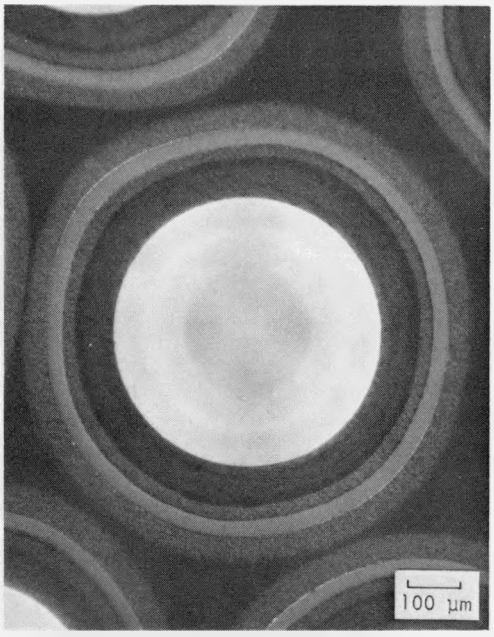

MP75019-2 (d)

Fig. 3-3. Representative photomicrographs of TRISO coated ThO_2 particles from batch 6252-05-0160: (a, b) bright field, (c, d) polarized light

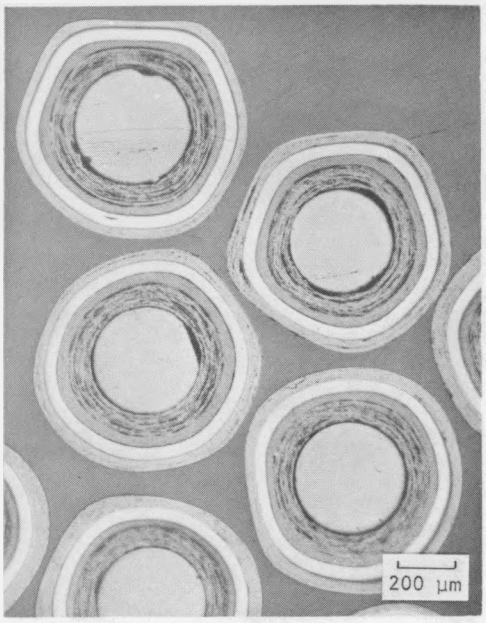

MP76001-1 (a)

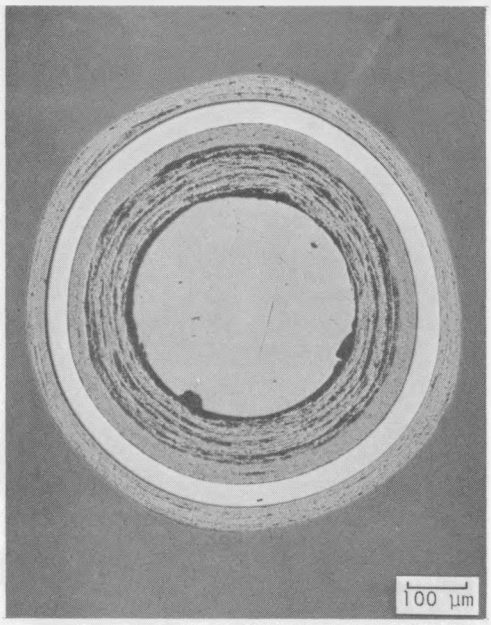

MP76001-4 (b)

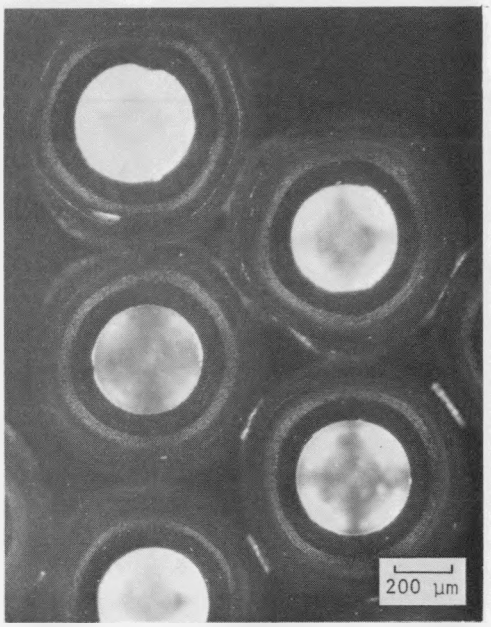

MP76001-2 (c)

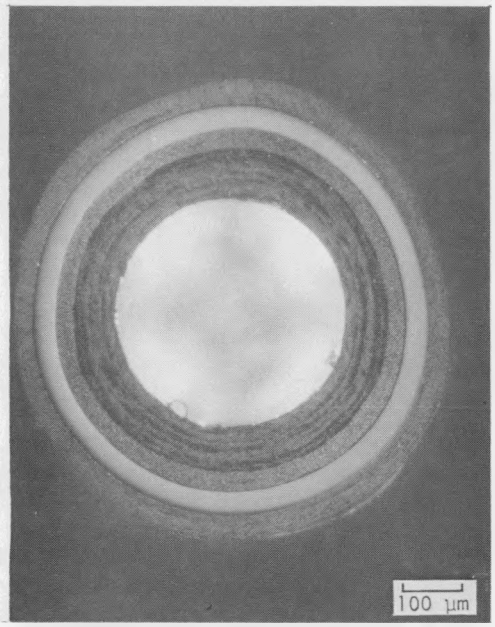

MP76001-5 (d)

Fig. 3-4. Representative photomicrographs of TRISO coated ThO_2 particles from batch 6252-06-0161: (a, b) bright field, (c, d) polarized light

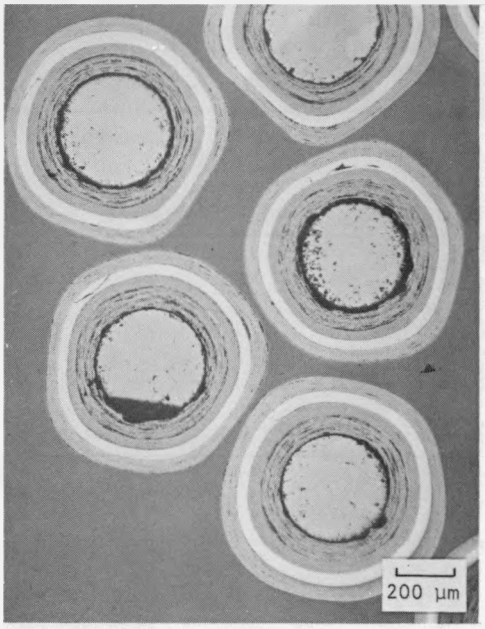

MP76002-1 (a)

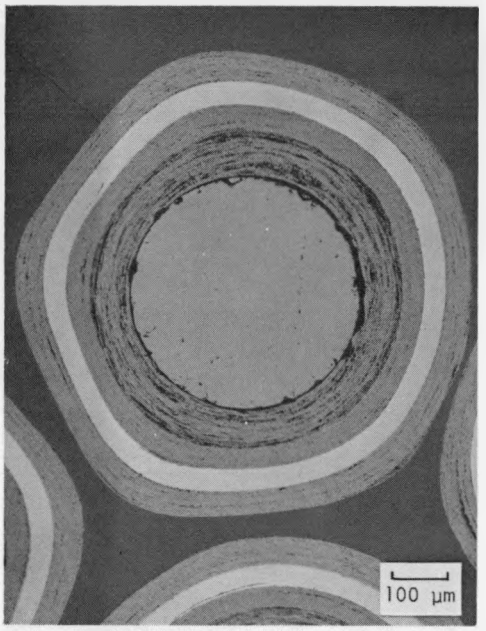

MP76002-4 (b)

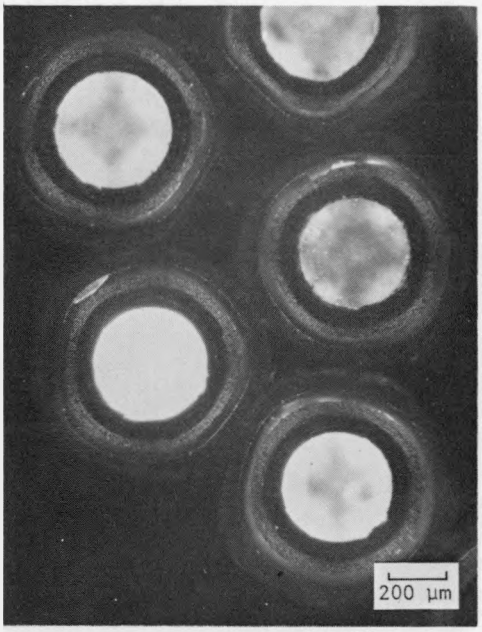

MP76002-2 (c)

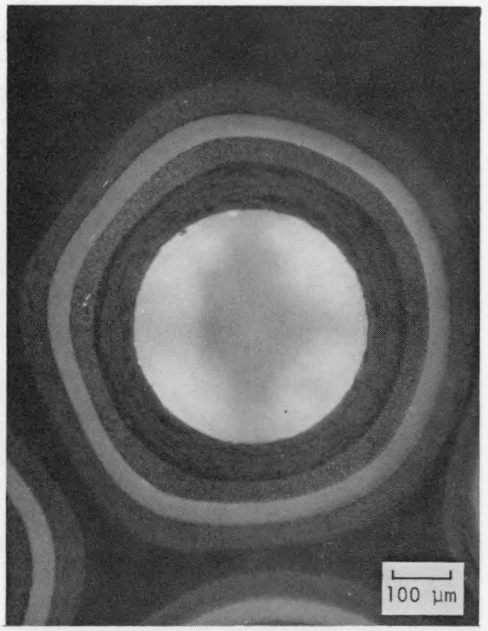

MP76002-5 (d)

Fig. 3-5. Representative photomicrographs of TRISO coated ThO_2 particles from batch 6252-06-0261: (a, b) bright field, (c, d) polarized light

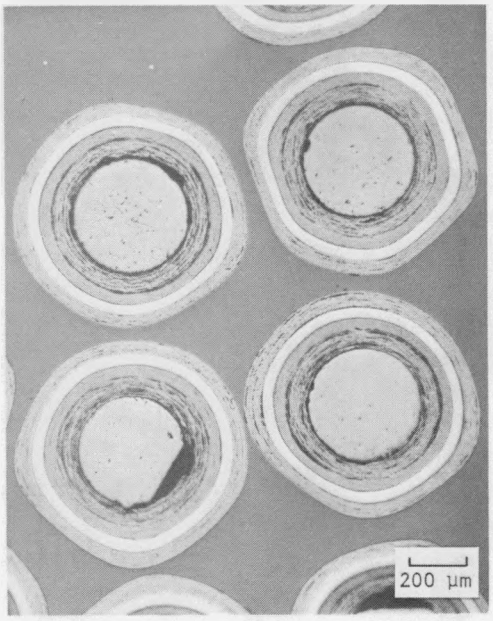

MP76003-2 (a)

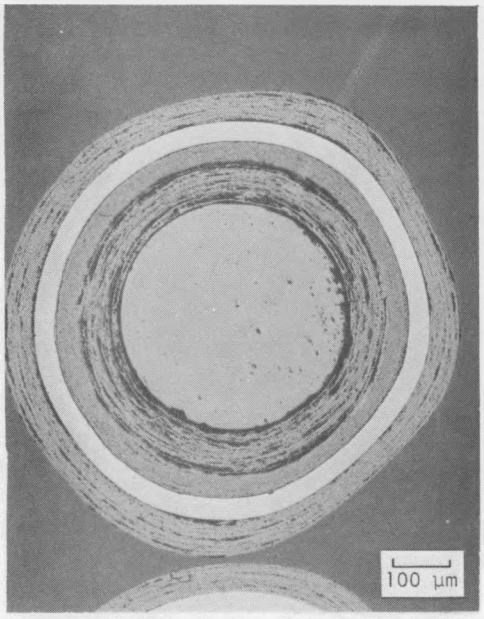

MP76003-5 (b)

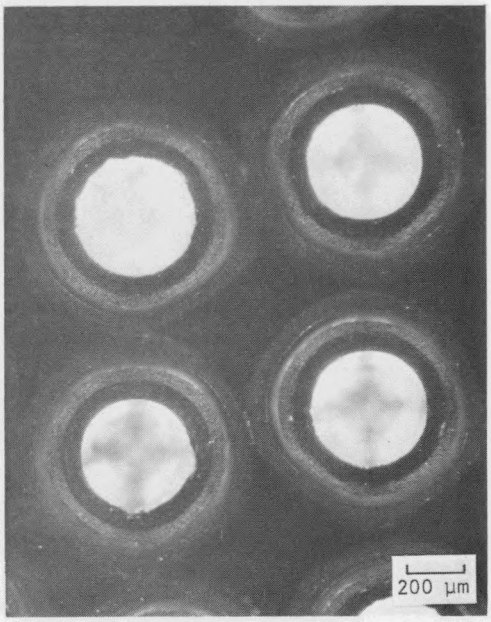

MP76003-1 (c)

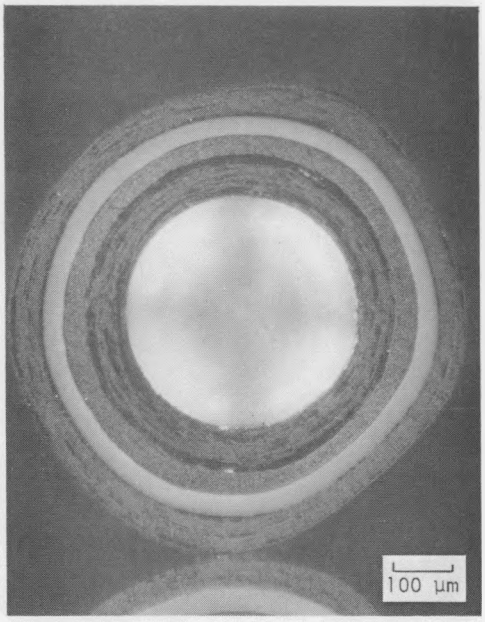

MP76003-4 (d)

Fig. 3-6. Representative photomicrographs of TRISO coated ThO_2 particles from batch 6252-07-0161: (a, b) bright field, (c, d) polarized light

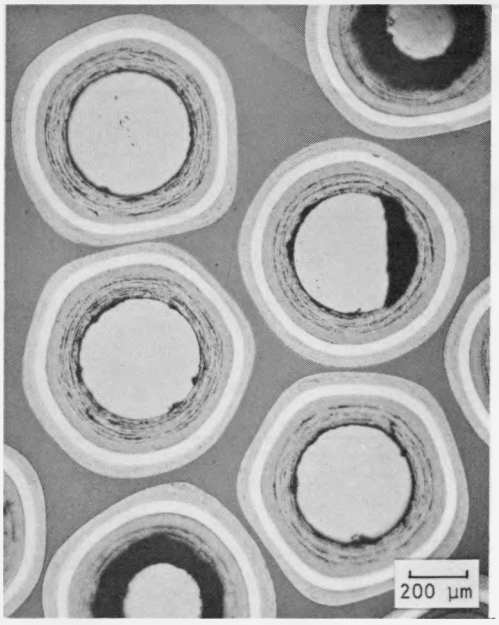

MP76004-1 (a)

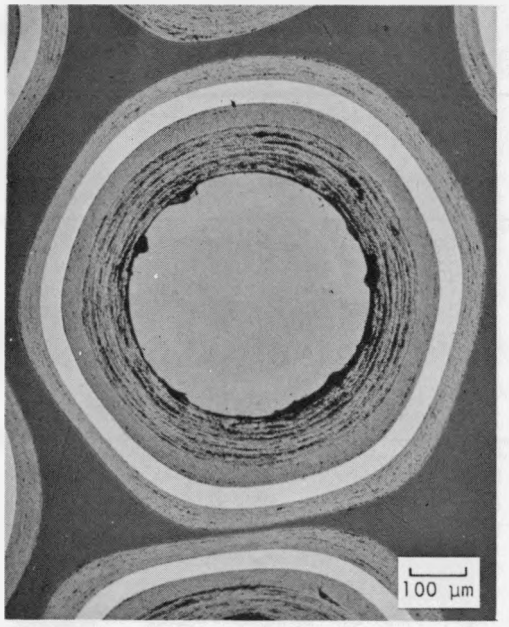

MP76004-4 (b)

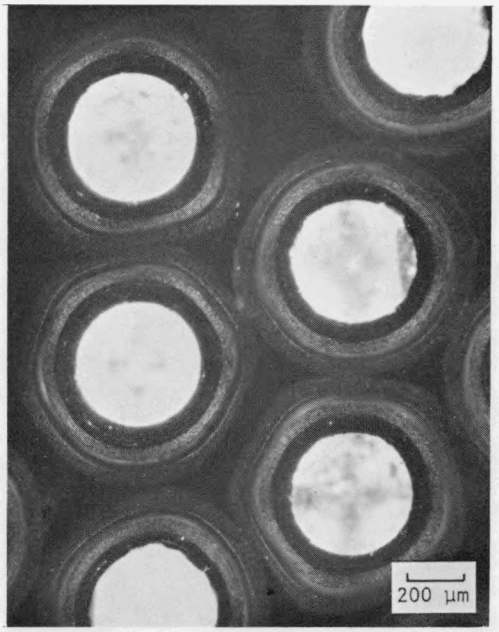

MP76004-2 (c)

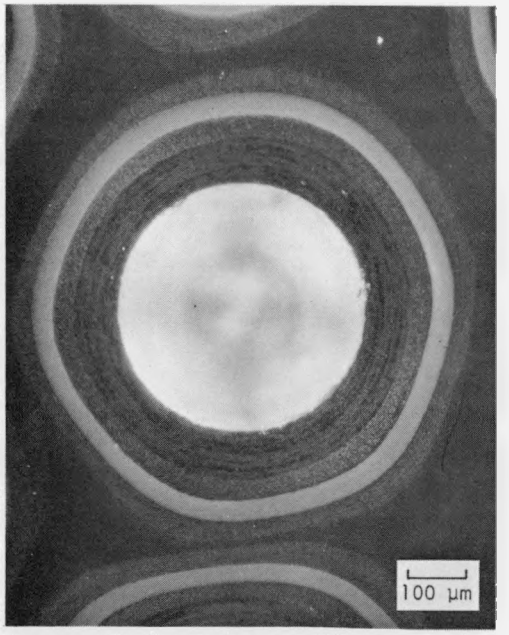

MP76004-5 (d)

Fig. 3-7. Representative photomicrographs of TRISO coated ThO_2 particles from batch 6252-07-0261: (a, b) bright field, (c, d) polarized light

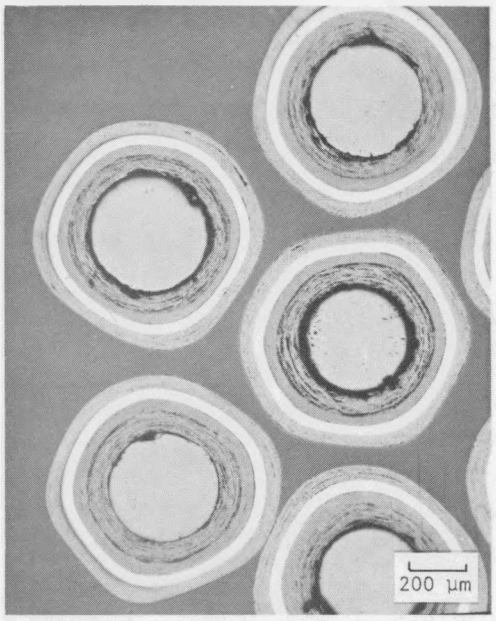

MP76005-1 (a)

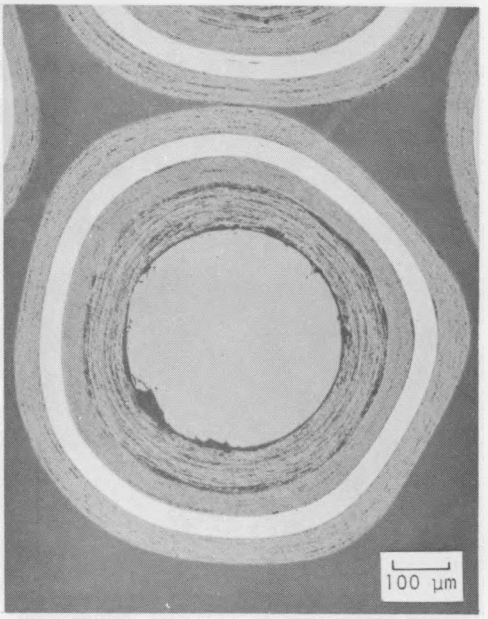

MP76005-5 (b)

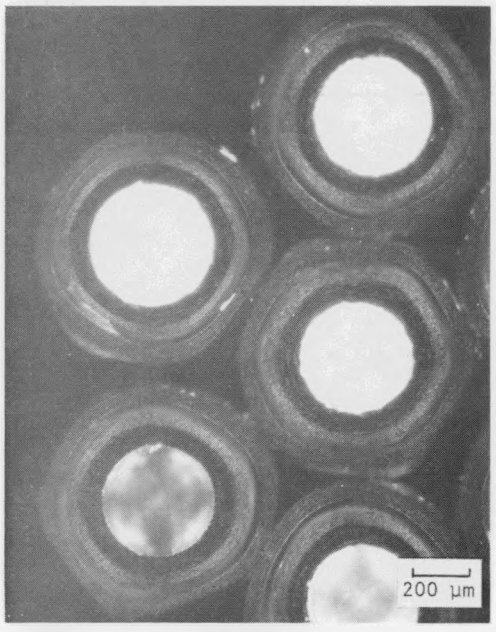

MP76005-2 (c)

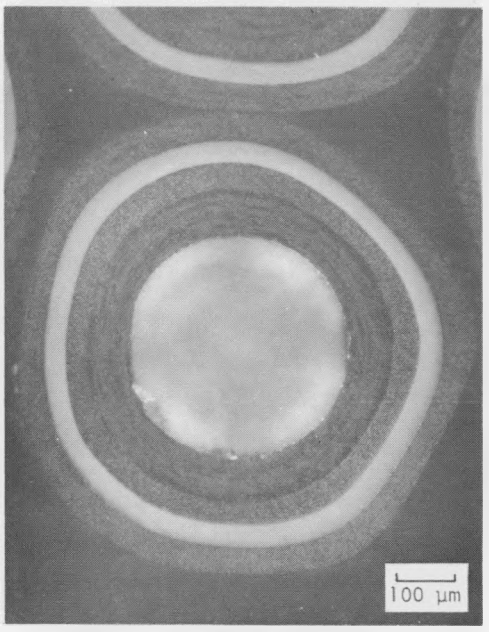

MP76005-7 (d)

Fig. 3-8. Representative photomicrographs of TRISO coated ThO_2 particles from batch 6252-08-0161: (a, b) bright field, (c, d) polarized light

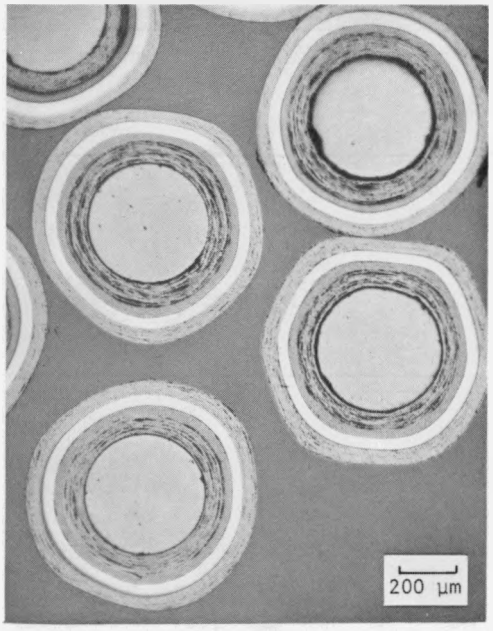

MP76006-1 (a)

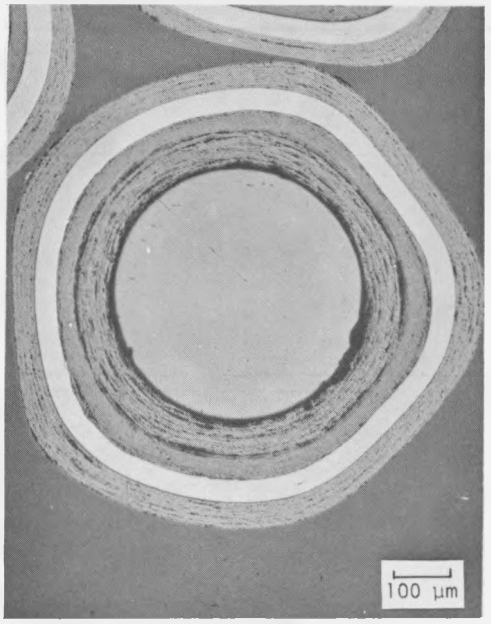

MP76006-7 (b)

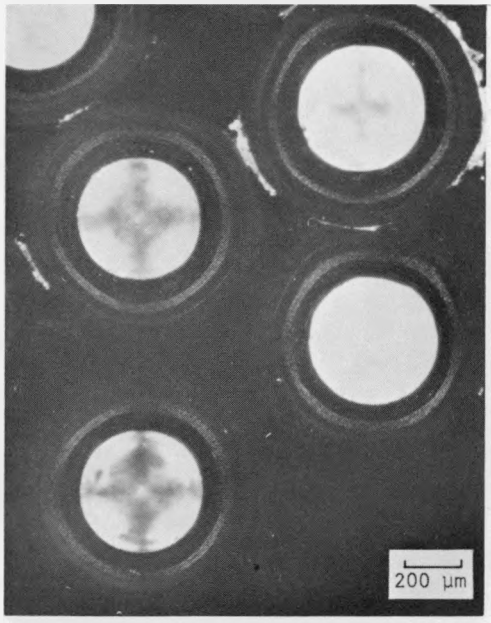

MP76006-2 (c)

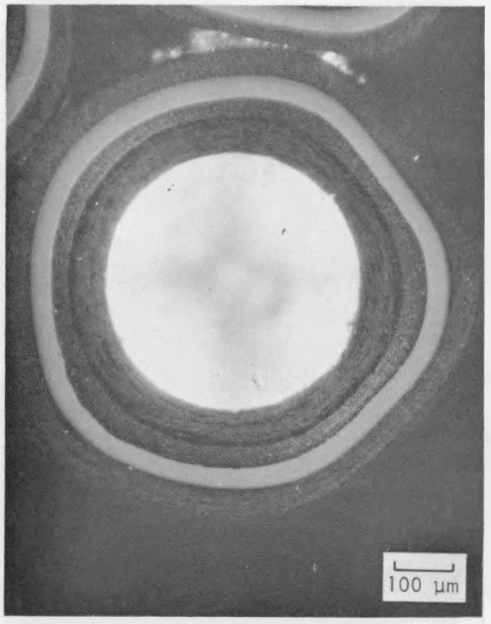

MP76006-8 (d)

Fig. 3-9. Representative photomicrographs of TRISO coated ThO_2 particles from batch 6252-09-0161: (a, b) bright field, (c, d) polarized light

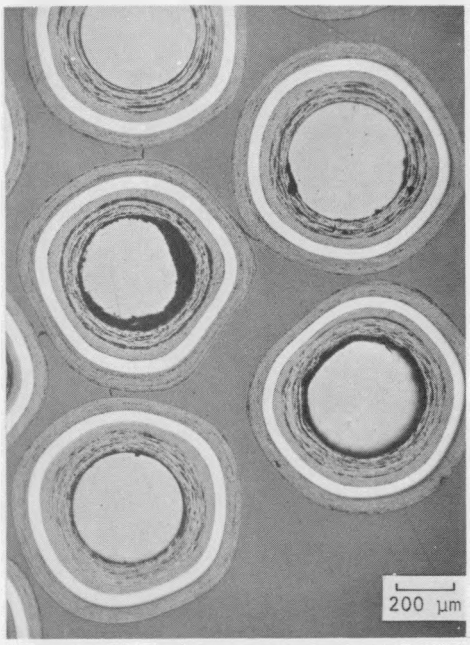

MP76007-1 (a)

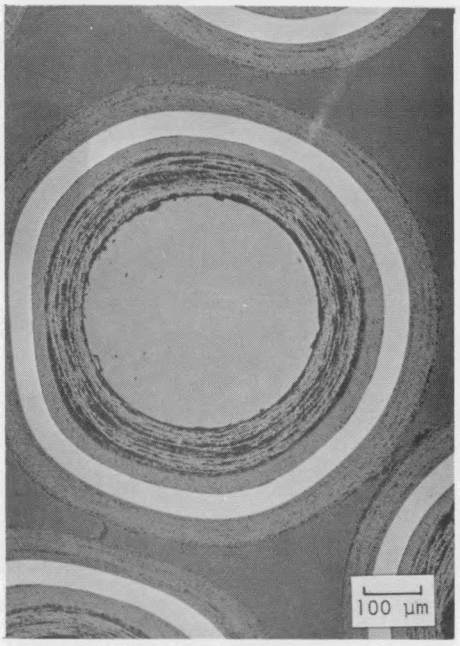

MP76007-4 (b)

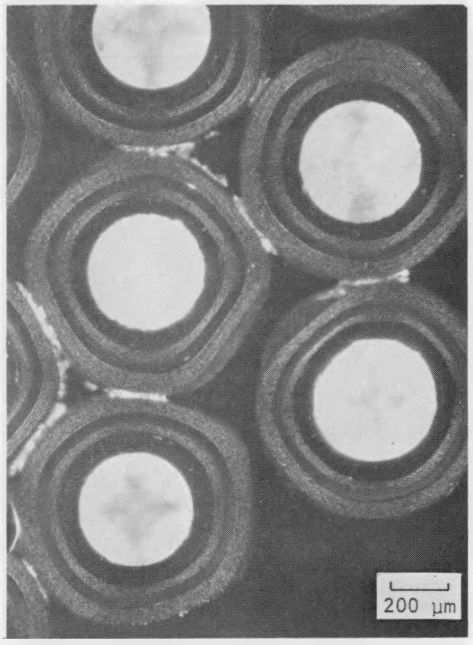

MP76007-2 (c)

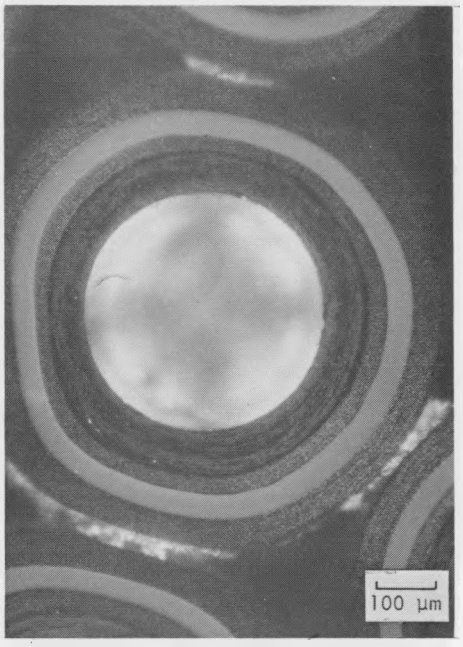

MP76007-5 (d)

Fig. 3-10. Representative photomicrographs of TRISO coated ThO_2 particles from batch 6252-10-0161: (a, b) bright field, (c, d) polarized light

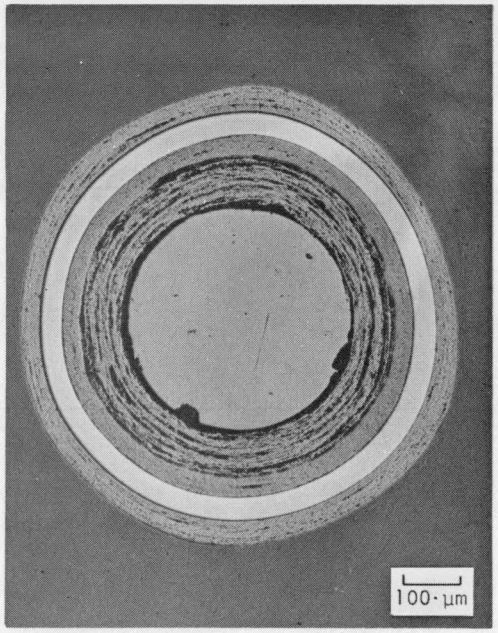

MP76001-4 (a)

Batch 6252-06-0161

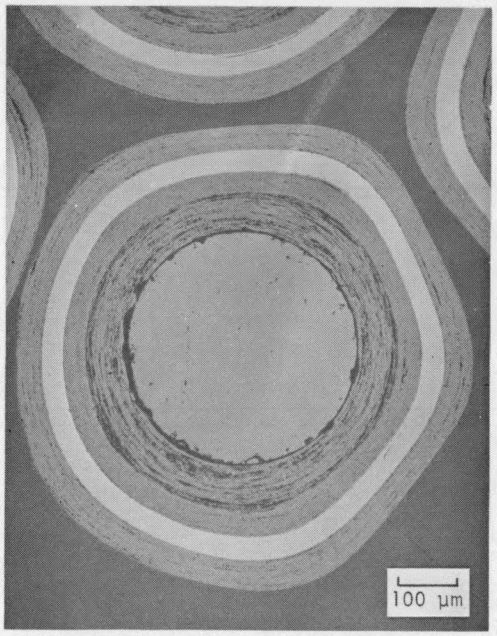

MP76002-4 (b)

Batch 6252-06-0261

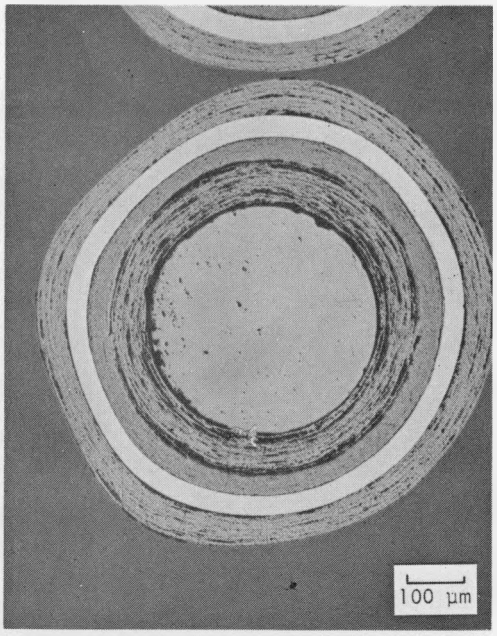

MP76003-5 (c)

Batch 6252-07-0161

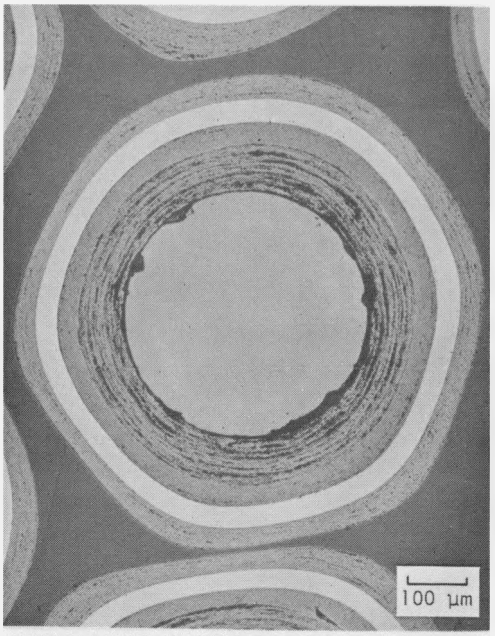

MP76004-4 (d)

Batch 6252-07-0261

Fig. 3-11. Representative photomicrographs of TRISO coated ThO_2 particles depicting different porosity structures in the OPyC layers: (a,c) laminated oriented porosity, (b,d) dispersed porosity

Fig. 3-12. Metallographic cross sections depicting representative morphology and size distribution of SiC flaws. SiC flaws are generic to all TRISO coated ThO_2 batches tested in HT-31 and HT-33. (Sheet 1 of 2)

(there was no photo printed on the page)

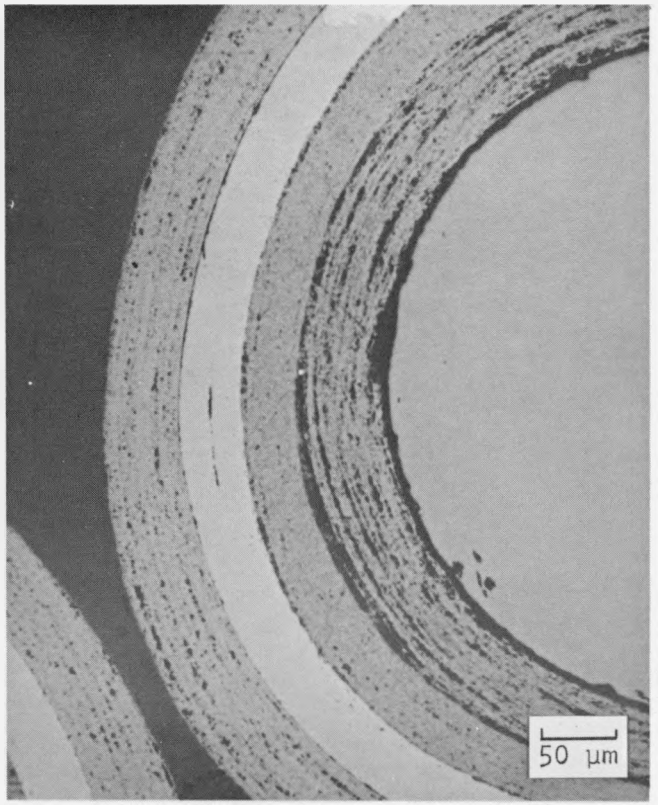

N76001-3

Batch No. 6252-07-020

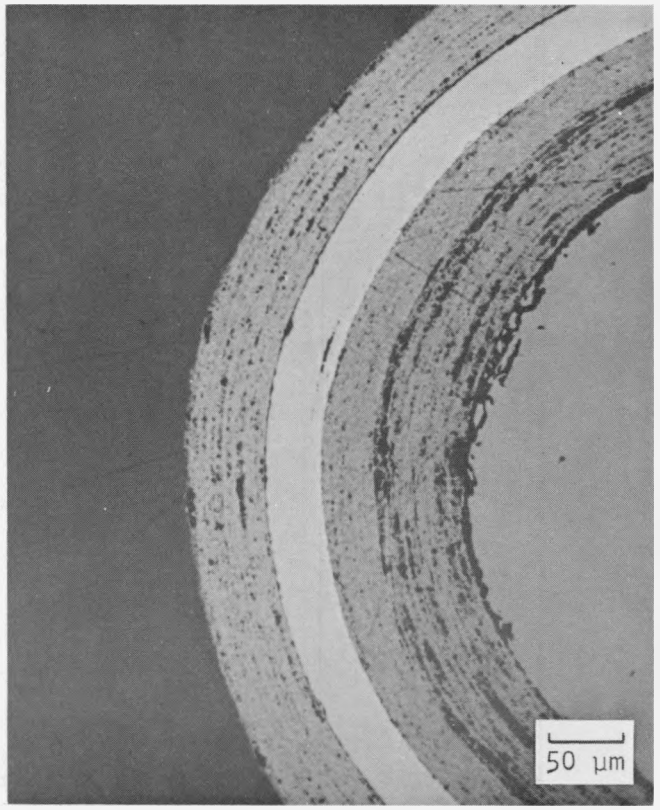

N76002-2

Batch No. 6252-07-020

Fig. 3-12. Metallographic cross sections depicting representative morphology and size distribution of SiC flaws. SiC flaws are generic to all TRISO coated ThO_2 batches tested in HT-31 and HT-33. (Sheet 2 of 2)

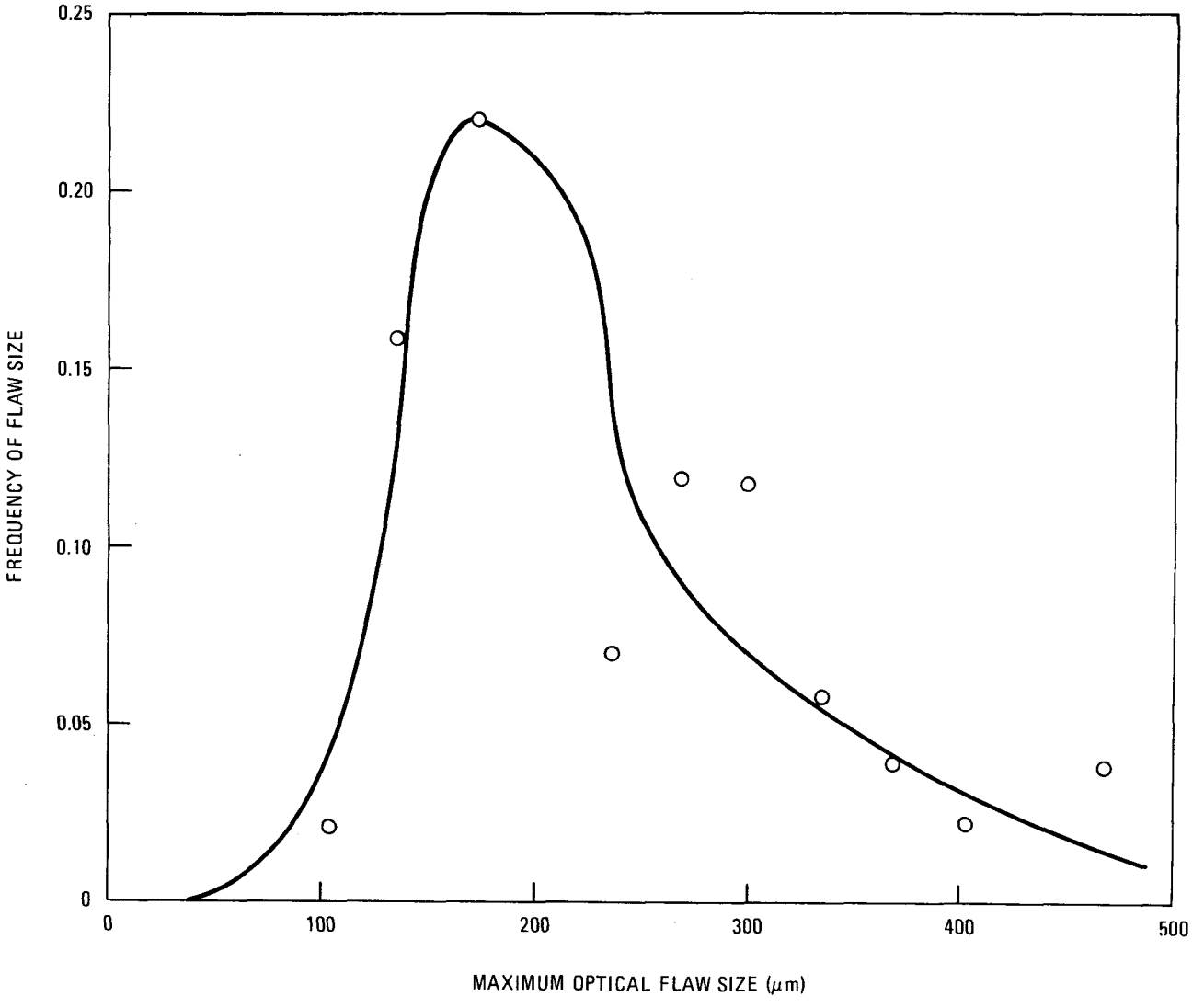

Fig. 3-13. Maximum optical flaw size distribution in defective SiC layers

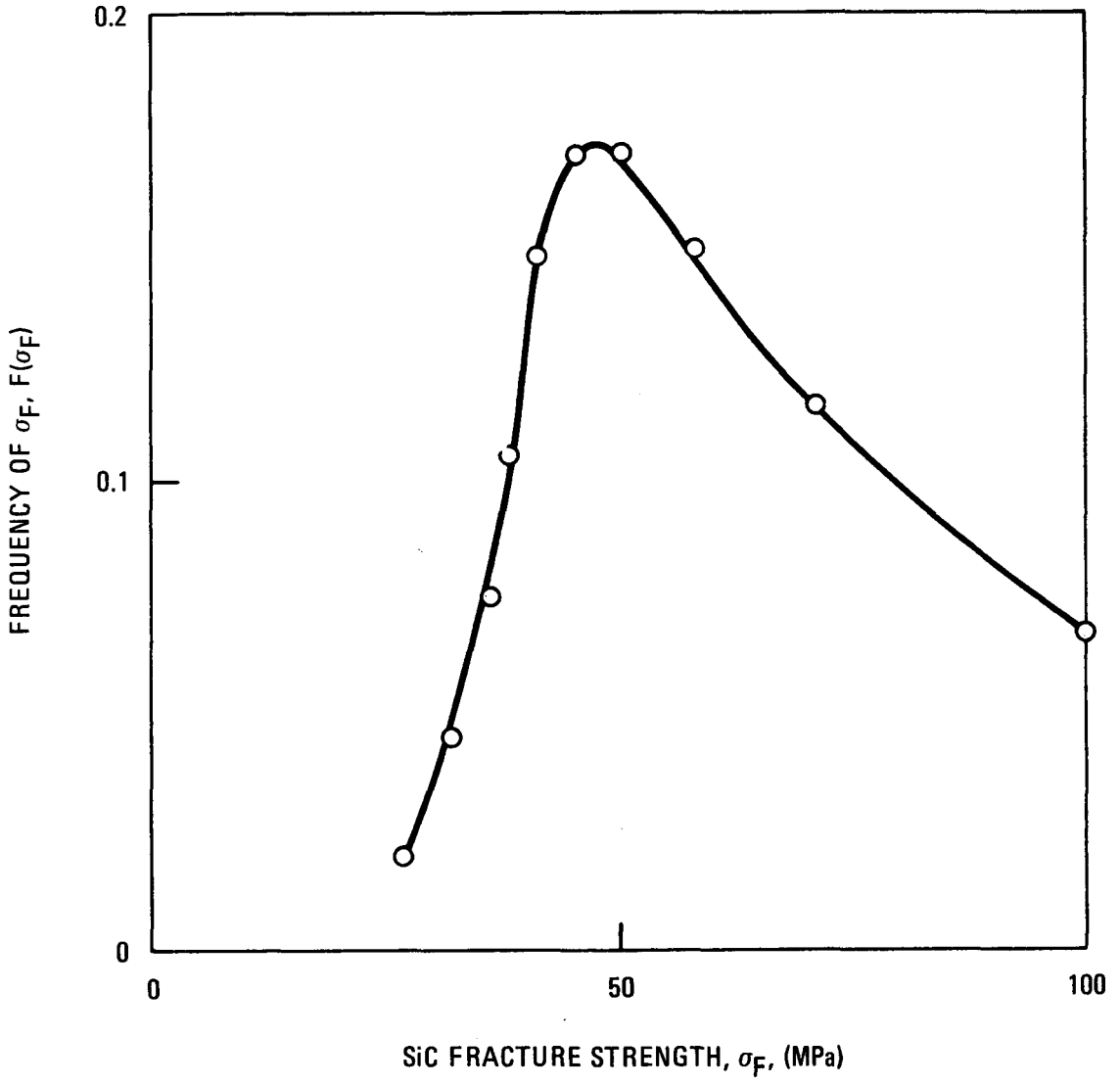

Fig. 3-14. Fracture strength distribution in TRISO coated ThO_2 particles based on the SiC flaw size distribution shown in Fig. 3-12

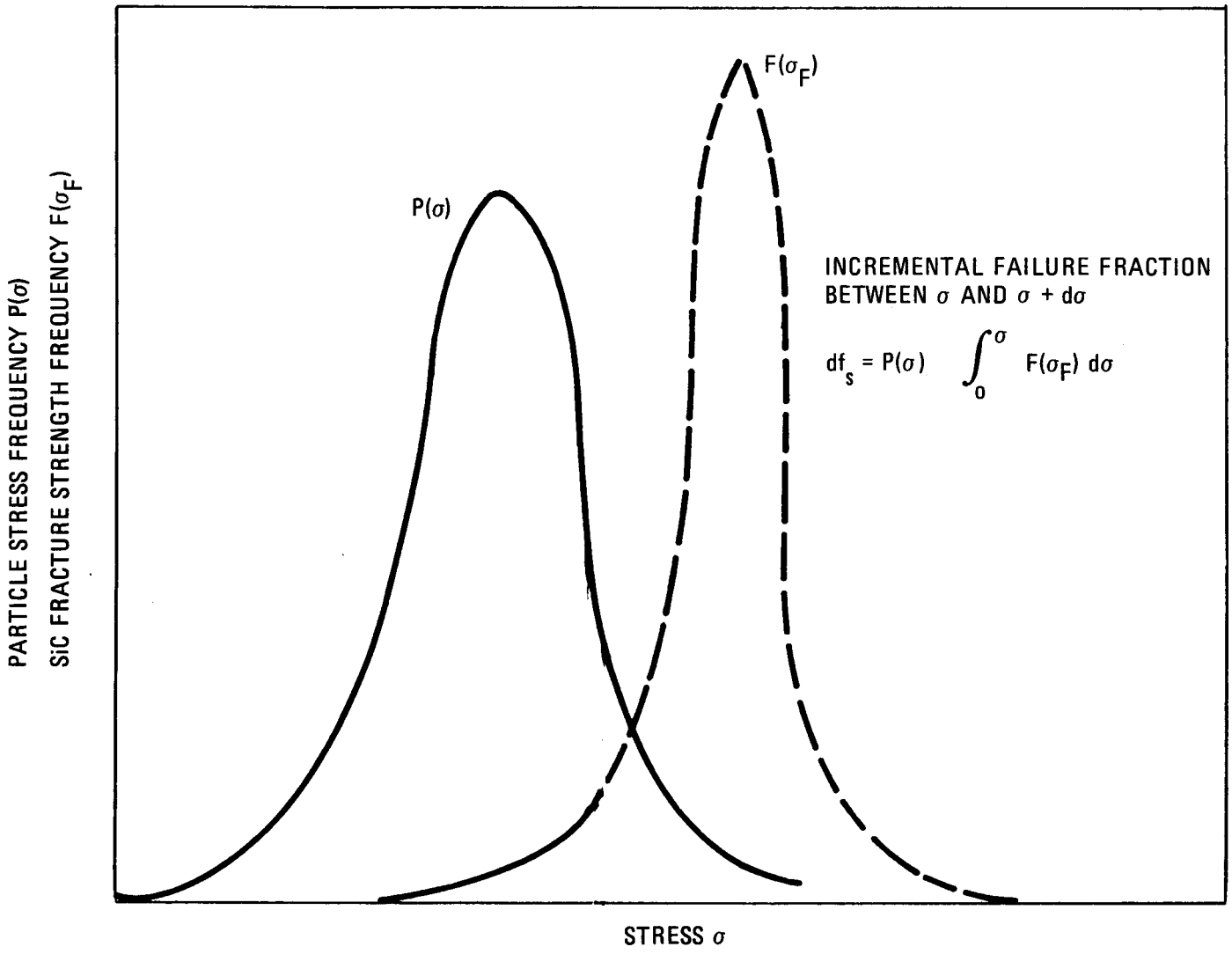

Fig. 3-15. Superposition of arbitrary particle stress and fracture strength distributions

4. BISO COATED ThO_2 PARTICLES

C. A. Young

4.1. OBJECTIVES

The two main objectives of the testing of BISO coated ThO_2 particles in capsule HT-33 are as follows:

1. Evaluate the irradiation performance of unbonded particles fabricated in the 240-mm-diameter pilot plant coater in accordance with performance criteria developed from particles of similar designs and coating properties fabricated in the prototype 127-mm-diameter coater. Fabricating fuel particles in the large coater is part of the planned processing scale-up and verification of applicability of previous specifications to the scaled-up process is desirable.

2. Define empirical relationships between the coating irradiation performance and the outer pyrocarbon (OPyC) coating variables of density, coating rate, diluent gas composition, and anisotropy. Also, aid in defining the permissible range of acceptable coating properties for the LHTGR product specification.

4.2. IRRADIATION CONDITIONS

The BISO fertile particle samples will occupy the top two magazines of the HT-33 capsule. (The bottom two magazines contain GA TRISO coated ThO_2 samples.) The irradiation conditions of the samples are given in Table 4-1. The surface temperatures of the graphite sample crucibles of the top magazine and the magazine adjacent to the top one are designed to be 900° and 1250°C, respectively. These graphite temperatures correspond to particle

temperatures of about 1200° and 1500°C, respectively. The low-temperature magazine samples will reach fluences of 5.1 to 8.1 x 10^{25} n/m^2 $(E > 29\ fJ)_{HTGR}$ and burnups of 7.2 to 10.3% FIMA. The fast fluences and the burnups for the high-temperature magazine are 9.2 to 10.2 x 10^{25} n/m^2 $(E > 29\ fJ)_{HTGR}$ and 11.4 to 12.4% FIMA.

4.3. COATED PARTICLE BATCHES AND SAMPLES

4.3.1. Description of Particle Batch Variables

Six ThO_2 BISO batches containing 500-μm kernels will be tested in the HT-33 capsule. All batches have similar dimensions. Five of the batches were fabricated in the large coater at different OPyC coating rates, diluent gases, and temperatures to obtain the desired OPyC coating densities and optical anisotropies (BAF_o values). Two OPyC coating rates (4 and 6 μm/min), two bulk densities (1.68 and 1.90 Mg/m^3), and a range of BAF_o values (1.04 to 1.08) will be tested in the large coater batches. The sixth batch, previously irradiated in capsules HT-28 and HT-29, was manufactured in the 127-mm-diameter coater and will be used as a comparison sample. Much of the present irradiation data is from batches coated in these smaller coaters. One sample from each batch was heat treated to 1650°C for 90 minutes in Ar to simulate the fuel rod heat treatment cycle, which affects important coating parameters. Presently, the expected fuel rod heat treatment is 1650°C and the maximum allowable time at temperature is 90 minutes for the LHTGR. Two of the large coater samples were not heat treated and these will be used as a comparison. The test matrix for the large coater ThO_2 BISO batches is shown in Fig. 4-1 and the variables and design irradiation conditions of each sample are given in Table 4-1.

The original test matrix had a wider range of bulk densities (1.80 to 1.92 Mg/m^3) at the two coating rates (Ref. 4-1). Ideally, each batch was to have an OPyC coating BAF_o of ≤ 1.04 and a fission gas release of $\leq 3 \times 10^{-5}$ R/B (Kr-85m). At the time the ThO_2 BISO batches were required for the HT-33 capsule, the state of the art of large coater fabrication was such that either a low BAF_o could be obtained with a low-density OPyC

coating which was permeable to fission gases (high fission gas release), or a high-density OPyC coating batch with a high BAF_o and low fission gas release could be made. Since the fission gas release for fuel particles had to be low, the first group of batches selected for the capsule had a high bulk density ($\sim$1.90 Mg/m^3) and a high BAF_o (1.06 to 1.08). While these batches were being evaluated, coating development continued and the diluent gas was changed from N_2 or Ar to H_2. This change resulted in batches with a low OPyC coating density having both the desired BAF_o and fission gas release. The H_2 dilution was used to reduce the hydrocarbon decomposition rate, and a more uniform microstructure with less interconnected porosity was formed. Two batches that were coated using H_2 dilution were evaluated and selected for capsule HT-33.

4.3.2. Fabrication of Batches

Five of the ThO_2 BISO batches were manufactured using HTGR pilot plant processes. All kernels and particles were manufactured to the specifications in Ref. 4-2. The 500-μm kernels were made from ThO_2 powder derived from a steam denitrated thorium nitrate solution. A gel and then a broth were prepared from the ThO_2 powder. The broth was fed into the drop column where it was spheroidized into uniform droplets and gelled in ammonia gas. The gelled spheres were dried in air at 150°C and sintered in a vertical tube furnace at a minimum temperature of 1300°C. The kernels were coated in the pilot plant coater which had an internal diameter of 240 mm. The fabrication conditions for the batches are given in Table 4-2. The buffer and OPyC coatings were deposited in the fluidized bed from the coating gases acetylene and propylene/acetylene (mixed gases), respectively. The diluent gas for the OPyC coating was N_2 for three of the batches and H_2 for two batches. The gases were introduced into the coater through a cone-shaped gas distributor. After the OPyC coating was deposited for each batch, the coater was cooled to about 1100°C and the particles were dumped into a hopper and covered with an inert atmosphere until the particles had cooled.

Parent batch 6542-27-015, a comparison batch, was fabricated before the pilot plant was set up. Three main items distinguish this batch from the other five batches. The ThO_2 powder used in the preparation of the sol was produced by calcination of thorium oxalate instead of steam denitration of a thorium nitrate solution. The initial load size of kernels was much smaller than the other batches (2 kg versus 13 or 20 kg) and the coater had an inside diameter of 127 mm instead of 240 mm.

4.3.3. Preparation of Capsule Samples

Each parent batch was evaluated and prepared for the HT-33 capsule as shown in Fig. 4-2. The batches were inspected according to the specifications in Refs. 4-2 and 4-3 in order to characterize the batch prior to irradiation. All the large coater batches were also heat treated at 1650°C for 90 minutes in Ar, and selected properties were measured on these samples. After characterization of the parent batch, a sample of the batch was sieved using a 790-μm BMC MicroMesh screen and a 833-μm Tyler screen to obtain the size fraction which passed through the smaller screen and remained on the larger screen. The sieved fraction was placed in a constant density liquid column and the particles which were suspended in the liquid were separated out. The separated fraction was heated in vacuum at 1400°C for 60 minutes to ensure volatilization of the liquid used for density separation. Part of the heated sample was annealed at 1650°C for 90 minutes in Ar to simulate the fuel rod heat treatment cycle.

After heat treatment of the particle samples, final preparation was done. The Th content (g Th/g particles) was calculated for the density-separated samples based on the densities and dimensions of the particle components and the weight fraction of Th in the kernel. The required thorium loadings (g Th) per position were obtained from ORNL, and the number of particles per position was calculated from the above data. After the particles were counted out for each position, the sample was radiographed and packaged for shipment to ORNL. The radiograph plate numbers for the samples are listed in Table 4-1.

4.3.4. Properties

All parent batches and capsule samples were extensively evaluated and characterized prior to irradiation. The results of the quality control analysis are presented in Tables 4-3 through 4-6. The HTGR fuel specifications (Ref. 4-3) and the batch properties which did not meet these specifications are given in Tables 4-7 and 4-8. Representative photographs of a microradiograph, macroscopic view, and metallographic cross section of coated particles from each parent batch are shown in Figures 4-3 through 4-8.

Certain properties were measured on the coated particles at different stages of preparation. The following items were measured on the parent batches: density, shape, and impurities of the kernels; buffer density, bulk (Ref. 4-4) and liquid gradient OPyC density, BAF_o (Ref. 4-4), faceting, and accessible porosity [measured by mercury intrusion (see Ref. 4-4)]; and the impurities, defective fraction, exposed thorium, and fission gas release of the total coated particles. The OPyC coating density, BAF_o, and accessible porosity and the fission gas release of the heat-treated samples were reported from the heat-treated parent batch data (unless data were not available). The total coated particle density and the Th content were obtained from the screened and density-separated fraction as shown in Fig. 4-2. Finally, the dimensions of the particle components and the OPyC coating rate were measured or calculated for the capsule test samples.

The three most significant property variables being tested in the HT-33 capsule are the OPyC coating rate, BAF_o, and density. The following discussions pertain mainly to the large coater batches. The two mean coating rates were approximately 4 and 6 μm/min, which are within the specification limits of Ref. 4-3 and meet the recommended mean coating rate based on the recently completed postirradiation examination of capsules P13R and P13S (Ref. 4-5). The three large coater batches fabricated without the H_2 diluent had mean OPyC coating BAF_o values of $\geq$1.06 and liquid gradient densities of about 1.90 Mg/m^3. The postirradiation results in Ref. 4-5 reveal that the ThO_2 BISO

particles which performed the best had an OPyC coating density of 1.85 to 1.95 Mg/m^3, a batch mean BAF_o of <1.04, and a batch mean coating rate of >3.5 μm/min. Based on these data, the three large coater batches fabricated without H_2 diluent may have high OPyC coating failure during irradiation because of the high BAF_o values. The other two large coater batches, which were fabricated with H_2 diluent, had mean BAF_o values of 1.038 and 1.042; these values are close to the recommended values (Ref. 4-5). However, the OPyC coating density (∿1.75 Mg/m^3) was lower than the recommended values of Ref. 4-5. Two mixed gas batches which had low OPyC densities in P13R and P13S unbonded particle tests were visually intact but were permeable to fission gases after irradiation. Also, the strength of the OPyC coating is reduced with decreasing density at constant crystallite size (Ref. 4-6). The irradiation of the H_2 diluted batches will show if the low OPyC density batches will retain the fission gases and if they will be strong enough to withstand the internal gas pressure buildup. (It should be noted that the BAF_o values were measured at GA with an optical anisotropy unit developed by ÖSGAE Seibersdorf, Austria. The equipment is sensitive to the condition of the equipment itself, especially the light source and photomultiplier tube, and the polished particle sample. All the batches except parent batch 6542-27-015 were measured about the same time and, therefore, these BAF_o values are reliable relative to each other.) In conclusion, a range of OPyC coating density and BAF_o values will be tested in the large coater batches having conservative coating rates to determine the effect of these two variables on the irradiation performance of the BISO particles.

The condition of the total coated particle was characterized by radiography, liquid acid leach, thorium hydrolysis, and fission gas release. No defective particles were detected in the parent batches or capsule test samples by radiography. The LHTGR fuel specification (Ref. 4-3) does not give a coated particle specification for thorium contamination, which can be measured by leach and hydrolysis tests, but the fuel rod specification is $\leq 1 \times 10^{-4}$ g exposed Th/g total Th. All of the batches except one met this requirement and most batches were much lower than the limit. Batch 6542-40-015 had a leach value of 5×10^{-4} g Th/g Th. This value was

probably not an accurate indication of the heavy metal contamination because both the hydrolysis and fission gas release values were very low. The high leach value was a result of either the sample being contaminated during the measurement or the OPyC coating being attacked by the acid leach. The latter is most likely because the batch was leached for a long time (24 hours) to ensure dissolution of any exposed ThO_2 kernels and it had the lowest OPyC coating density. Although fission gas release is not a specification item (Ref. 4-3) for coated particles, the specification is $\leq 3 \times 10^5$ R/B for Kr-85m at 1100°C for initial cores, blends, and reload segments. Two of the N_2-diluted coated particle batches were above this limit. Even though the OPyC density was high, these batches may be slightly permeable to fission gases since the exposed Th was low (low contamination).

A comparison of the as-coated and heat-treated parent batches is presented in Table 4-9. A sample of each of the large coater batches was annealed at 1650°C for 90 minutes in Ar for a QC analysis. As explained previously, the heat treatment of the HT-33 samples is more realistic of the condition of the particles in a fuel rod. The results for the heat-treated batches are consistent with the work done by Stevens (Ref. 4-7) and Kaae (Ref. 4-8). The liquid gradient density of the OPyC coating increased and the coating thicknesses decreased slightly for most of the batches. It is interesting to note that the BAF_o values of the batches coated using N_2 diluent increased significantly after heat treatment but the BAF_o values for the batches coated using H_2 diluent did not show this increase. The reason for this is not known; however, it may be related to high-density coatings being more responsive to annealing than low-density coatings rather than the diluent gas. Kaae has also shown that the strength of the annealed OPyC coatings is lower than that of as-coated OPyC coatings for high-density samples. The combination of decrease in strength and increase in anisotropy may cause higher particle failure in the heat-treated batches in comparison with the as-coated batches, especially for the very high-density batch (6542-41-015).

The properties of the ThO_2 BISO coated particle batches before and after the screening and density separation (no final heat treatment) are compared

in Table 4-10. The purpose of the sample preparation was to obtain a sample which had about the same mean property values as the parent batches but lower standard deviations. Consequently, the confidence in the test results is improved when relating total particle or coating performance to a given range of particle variables. The results of the sample preparation were that the standard deviations of the kernel diameter, OPyC coating thickness, and the total particle diameter of the daughter batches were sometimes higher rather than lower than the parent batches. The sieved buffer thickness standard deviation was consistently lower than the parent batches. The standard deviation of the kernel diameter did not change much since it was low to begin with (kernels very uniform in size). It was surprising that the particle diameter standard deviation of two of the sieved batches was about the same as the parent batch because the screening should have decreased the standard deviation by removing the smallest and largest particles. The actual diameter distribution of these two sieved samples showed that there were some very small particles in the screened fraction, which indicated that the screening operation was inefficient. However, the diameter standard deviations of the capsule particle samples from these two sieved fractions were lower than the parent batches. A comparison of Tables 4-5 and 4-10 shows that all the test samples had approximately the same mean kernel diameter and mean buffer and OPyC coating thicknesses and that the standard deviations of the buffer thickness were lower than the parent batches. These results, therefore, will facilitate the analysis of particle performance including the evaluation of the OPyC coating variables of density, coating rate, and anisotropy.

REFERENCES

4-1. Harmon, D. P., W. J. Kovacs, and C. A. Young, "Irradiation Test Plan for HFIR Experiments HT-31 and HT-33," General Atomic unpublished data, May 14, 1976.

4-2. "Fuel Specification for Irradiation Experiments," General Atomic unpublished data, April 5, 1974.

4-3. "HTGR Fuel Product Specification," Issue B, General Atomic Report GA-A13464, January 21, 1976.

4-4. "HTGR Fuels and Core Development Program Quarterly Progress Report for the Period Ending May 31, 1976," ERDA Report GA-A13941, General Atomic Company, June 30, 1976.

4-5. Scott, C. B., D. P. Harmon, and J. F. Holzgraf, "Postirradiation Examination of Capsules P13R and P13S," General Atomic Report GA-A13827, to be published.

4-6. Kaae, J. L., "Relations Between the Structure and Mechanical Properties of Fluidized-Bed Pyrolytic Carbons," Gulf General Atomic Report GA-10156, June 1, 1970.

4-7. Stevens, D. W., "Annealing of Isotropic Pyrolytic Carbons Formed Below 1500°C," Gulf General Atomic Report GA-10448, June 13, 1971.

4-8. Kaae, J. L., "The Effect of Annealing on the Microstructure and the Mechanical Properties of Poorly Crystalline Isotropic Pyrolytic Carbons," Gulf General Atomic Report Gulf-GA-A10868, October 18, 1971.

TABLE 4-1
IDENTIFICATION, VARIABLES, AND DESIGN IRRADIATION CONDITIONS OF THE BISO COATED FUEL SAMPLES FOR HT-33 CAPSULE

Sample Number[a]	Radiographic Plate Number of Sample	Variables: Process: Coater Size (mm)	Variables: Process: Initial Load Size (kg)	Variables: Process: OPyC Coating Diluent Gas	Variables: OPyC Coating: Density (Mg/m^3): Liquid Gradient	Variables: OPyC Coating: Density (Mg/m^3): Bulk	Variables: OPyC Coating: Coating Rate (μm/min)	Variables: OPyC Coating: BAF_o	Variables: Capsule Sample Heat-Treatment Condition: As-Coated	Variables: Capsule Sample Heat-Treatment Condition: 1650°C[b]	Design Irradiation Parameters: Capsule Position[c]	Design Irradiation Parameters: Number of Particles In Sample	Design Irradiation Parameters: Fast Fluence ($\times 10^{25}$ n/m^2) (E>29 fJ)$_{HTGR}$	Design Irradiation Parameters: Burnup (% FIMA)	Required Fuel Loadings[d] (mg)
1200°C Magazine[e]															
6542-39-0161-001	LB450	240	20	N_2	1.98	1.92	3.9	1.079		X	2	38	5.1	7.2	23.4
6542-40-0161-001	LB459	240	13	H_2	1.74	1.67	5.8	1.043		X	4	41	5.8	7.8	23.4
6542-40-0261-001	LB445	240	13	H_2	1.77	1.70	5.8	1.038		X	5	41	6.0	8.2	23.4
6542-40-0260-001	LB442	240	13	H_2	1.77	1.69	5.6	1.038	X		7	41	6.6	8.8	23.4
6542-27-0161-001	LB386	127	2	Ar	1.86	1.78	4.2	1.041		X	8	40	6.8	9.1	23.4
6542-29-0261-001	LB432	240	20	N_2	1.96	1.89	4.4	1.081		X	10	39	7.4	9.6	23.4
6542-41-0161-001	LB438	240	13	N_2	2.02	1.93	5.5	1.081		X	11	40	7.6	9.6	23.4
6542-41-0160-001	LB435	240	13	N_2	2.00	1.93	5.6	1.060	X		13	40	8.1	10.3	23.4
1500°C Magazine[f]															
6542-29-0261-002	LB433	240	20	N_2	1.96	1.89	4.2	1.081		X	15	55	9.2	11.4	33.1
6542-27-0161-002	LB387	127	2	Ar	1.86	1.78	4.2	1.041		X	17	57	9.5	11.7	33.1
6542-41-0161-002	LB439	240	13	N_2	2.02	1.93	5.5	1.081		X	18	56	9.6	11.8	33.1
6542-41-0160-002	LB436	240	13	N_2	2.00	1.93	5.4	1.060	X		20	56	9.8	12.0	33.1
6542-39-0161-002	LB451	240	20	N_2	1.98	1.92	4.1	1.079		X	21	54	9.9	12.1	33.1
6542-40-0161-002	LB460	240	13	H_2	1.74	1.67	5.7	1.043		X	23	58	10.0	12.2	33.1
6542-40-0261-002	LB446	240	13	H_2	1.77	1.70	5.6	1.038		X	24	58	10.1	12.3	33.1
6542-40-0260-002	LB443	240	13	H_2	1.77	1.69	5.7	1.038	X		26	58	10.2	12.4	33.1

[a] In the order in which they are located in the capsule.

[b] Heat treated at 1650°C for 90 minutes in Ar.

[c] The number designates the axial position in capsule; the numbers increase consecutively toward the bottom of the capsule.

[d] Obtained from ORNL.

[e] The top magazine in capsule HT-33.

[f] Located directly below the top magazine.

TABLE 4-2
FABRICATION CONDITIONS OF BISO COATED BATCHES FOR HT-33 CAPSULE

Parent Batch Number[a]	Coater Size[b] (mm)	Initial Kernel Load Size (kg)	Buffer			Outer Isotropic							
			Coating Rate (μm/min)	Coating Gas	Diluent and Carrier Gas	Coating Rate (μm/min)			Coating Gas	Coating Gas Ratio (C_2H_2/C_3H_6)	Diluent Gas	Hydrocarbon/ Hydrocarbon + H_2 Ratio	Temperature of Bed/Control (°C)
						Mean	Minimum[c]	Maximum[d]					
6542-27-015	127	2	18.6	C_2H_2	Ar	4.6	3.6	5.5	C_2H_2/C_3H_6	1.17	Ar	1.0	1300/(e)
6542-29-025	240	20	9.0	C_2H_2	Ar	4.3	3.3	5.4	C_2H_2/C_3H_6	0.43	N_2	1.0	1335/1400
6542-39-015	240	20	8.6	C_2H_2	Ar	4.1	2.9	5.2	C_2H_2/C_3H_6	0.43	N_2	1.0	1315/1375
6542-40-015	240	13	13.6	C_2H_2	Ar	5.8	4.4	7.2	C_2H_2/C_3H_6	0.43	H_2	0.41	(e)/1540
6542-40-025	240	13	13.9	C_2H_2	Ar	5.8	4.6	7.2	C_2H_2/C_3H_6	0.43	H_2	0.50	(e)/1525
6542-41-015	240	13	13.0	C_2H_2	Ar	5.8	4.4	7.2	C_2H_2/C_3H_6	0.43	N_2	1.0	1300/1360

[a]The capsule samples have the number 6 instead of 5 for the ninth number, i.e., batch 6542-27-015 is the parent batch for sample 6542-27-0161-001.

[b]The coater had a cone gas distributor.

[c]Determined by dividing the lower 95 percentile limit of the thickness by the coating time.

[d]Determined by dividing the upper 95 percentile limit of the thickness by the coating time.

[e]Not determined.

TABLE 4-3
GENERAL DESCRIPTION OF BISO COATED PARTICLES FOR HT-33 CAPSULE

Sample Batch Number	Heat Treatment	Kernel Diameter[a] (μm)	Coatings										Total Coated Particle				
			Coater Size (mm)	Buffer		Outer Isotropic						Total Coating Thickness[a] (μm)	Diameter[a] (μm)	Density[h] (Mg/m^3)	Th Content[i] (wt %)	Exposed Th[c,j] (kg Th/kg Th)	Fission Gas Release[d,k]
				Thickness[a] (μm)	Density[b,c] (Mg/m^3)	Thickness[a] (μm)	Density[d] (Mg/m^3) Sink Float[e]	Density[d] (Mg/m^3) Bulk[f]	Coating Rate[a] (μm/min)	BAF_o[d,g]	Fabrication Diluent Gas						
6542-27-0161-001	Yes	500	127	87	1.09	75	1.86[1]	1.78[1]	4.2	1.041[m]	Ar	162	823	3.45	56.8	3.7×10^{-6}	3.4×10^{-6}[1]
-002	Yes	503	127	88	1.09	75	1.86[1]	1.78[1]	4.2	1.041[m]	Ar	164	829	3.45	56.8	3.7×10^{-6}	3.4×10^{-6}[1]
6542-29-0261-001	Yes	504	240	94	1.13	76	1.96	1.89	4.4	1.081	N_2	170	843	3.45	54.9	6.1×10^{-7}	6.1×10^{-5}
-002	Yes	503	240	93	1.13	72	1.96	1.89	4.2	1.081	N_2	166	833	3.45	54.9	6.1×10^{-7}	6.1×10^{-5}
6542-39-0161-001	Yes	508	240	86	1.13	71	1.98	1.92	3.9	1.079	N_2	156	821	3.61	58.9	4.5×10^{-7}	6.2×10^{-6}
-002	Yes	508	240	86	1.13	74	1.98	1.92	4.1	1.079	N_2	161	826	3.61	58.9	4.5×10^{-7}	6.2×10^{-6}
6542-40-0161-001	Yes	500	240	91	1.10	73	1.74	1.67	5.8	1.042	H_2	164	828	3.35	57.1	5.1×10^{-4}	$<1.4 \times 10^{-6}$
-002	Yes	502	240	93	1.10	71	1.74	1.67	5.7	1.042	H_2	164	827	3.35	57.1	5.1×10^{-4}	$<1.4 \times 10^{-6}$
6542-40-0260-001	No	503	240	85	1.10	76	1.77	1.69	5.6	1.038	H_2	161	829	3.36	57.0	2.2×10^{-5}	3.6×10^{-6}
-002	No	500	240	88	1.10	77	1.77	1.69	5.7	1.038	H_2	164	826	3.36	57.0	2.2×10^{-5}	3.6×10^{-6}
6542-40-0261-001	Yes	500	240	89	1.10	78	1.77	1.70	5.8	1.038	H_2	168	832	3.39	57.0	2.2×10^{-5}	$<1.4 \times 10^{-6}$
-002	Yes	501	240	87	1.10	76	1.77	1.70	5.6	1.038	H_2	164	828	3.39	57.0	2.2×10^{-5}	$<1.4 \times 10^{-6}$
6542-41-0160-001	No	507	240	91	1.13	70	2.00	1.93	5.6	1.060	N_2	160	827	3.51	56.0	1.5×10^{-5}	4.2×10^{-5}
-002	No	505	240	88	1.13	68	2.00	1.93	5.4	1.060	N_2	155	817	3.51	56.0	1.5×10^{-5}	4.2×10^{-5}
6542-41-0161-001	Yes	503	240	92	1.13	69	2.02	1.93	5.5	1.081	N_2	161	825	3.54	56.0	1.5×10^{-5}	5.6×10^{-5}
-002	Yes	503	240	92	1.13	69	2.02	1.93	5.5	1.081	N_2	161	823	3.54	56.0	1.5×10^{-5}	5.6×10^{-5}

[a] Measured or calculated on capsule test samples.

[b] Determined by a mathematical calculation.

[c] Measured on as-coated parent batch.

[d] Measured on heat-treated parent batches, except where noted, for the heat-treated capsule test samples; otherwise the as-coated parent batches were measured.

[e] Measured by a liquid gradient technique.

[f] Calculated from the equation $\frac{1}{\rho_B} = \frac{1}{\rho_{SF}} + K(AP)$, where ρ_b = bulk density, ρ_{SF} = sink float density, K = constant, and AP = accessible porosity.

[g] Optical anisotropy measured using the Seibersdorf optical unit at GA using a 24-μm-diameter light spot at the center of the coatings.

[h] Density of density-separated fraction measured by liquid gradient technique.

[i] Calculated from parent batch densities and dimensions of density-separated fraction for particle components and the kernel composition.

[j] Determined by acid-leach test.

[k] Release rate/birth rate for Kr-85m at 1100°C; activated in linear accelerator.

[l] Values for as-coated parent batch; data not available for heat-treated parent batch.

[m] Sample heat treated at 1800°C for 1 hour in He for this QC measurement.

TABLE 4-4
KERNEL PROPERTIES OF BISO COATED PARTICLES FOR HT-33 CAPSULE

Sample Batch Number	Kernel Batch Number	Diameter[a] (μm)		Density[b,c] (Mg/m^3)	Shape[c,d] (%)	Impurities[c] (ppm-wt)					
		Mean	Standard Deviation			Fe	Cr	Ni	Na	Ca	Total[e]
6542-27-0161-001	4222-04-010	500	9.3	9.88	3	<25	<25	<25	<100	<200	171[f]
-002	4222-04-010	503	8.0	9.88	3	<25	<25	<25	<100	<200	171[f]
6542-29-0261-001	4222-07-0110	504	8.2	9.79	0	<10	<4	<8	<10	<10	613
-002	4222-07-0110	503	7.9	9.79	0	<10	<4	<8	<10	<10	613
6542-39-0161-001	4222-07-0130	508	5.6	9.79	0	<10	<4	<8	<10	<10	613
-002	4222-07-0130	508	8.6	9.79	0	<10	<4	<8	<10	<10	613
6542-40-0161-001	4222-07-0152	500	8.2	9.74	1	22	<4	<8	<10	<10	573
-002	4222-07-0152	502	9.8	9.74	1	22	<4	<8	<10	<10	573
6542-40-0260-001	4222-07-0143	503	11.5	9.76	1	12	<4	<8	<10	<10	253
-002	4222-07-0143	500	9.5	9.76	1	12	<4	<8	<10	<10	253
6542-40-0261-001	4222-07-0143	500	9.2	9.76	1	12	<4	<8	<10	<10	253
-002	4222-07-0143	501	9.6	9.76	1	12	<4	<8	<10	<10	253
6542-41-0160-001	4222-07-0111	507	10.6	9.73	1	16	<4	<8	<10	<10	713
-002	4222-07-0111	505	9.2	9.73	1	16	<4	<8	<10	<10	713
6542-41-0161-001	4222-07-0111	503	7.8	9.73	1	16	<4	<8	<10	<10	713
-002	4222-07-0111	503	9.2	9.73	1	16	<4	<8	<10	<10	713

[a] Kernels of capsule test samples measured by contact radiography.

[b] Measured using Hg porosimetry.

[c] Measured on parent kernel batches.

[d] Percent of kernels with a ratio of maximum diameter/minimum diameter $\geq$ 1.2 measured by contact radiography, measured on 200 kernels.

[e] The following impurities were measured by spectrographic analysis: Al, Ca, Cr, Mg, Na, Pb, Sr, B, Cd, Cu, Mn, Ni, Si, V, Ba, Fe, Mo, P, Sn, Zn, Be, Bi, Tl, except where noted.

[f] The following impurities were not measured: Be, Bi, Tl; however, Co was measured.

TABLE 4-5
COATING PROPERTIES OF BISO COATED PARTICLES FOR HT-33 CAPSULE

Sample Batch Number	Heat Treatment	Buffer				OPyC								
		Thickness[a] (μm)		Density[b,c] (Mg/m^3)	Faceting[c,d]	Thickness[a] (μm)		Density (Mg/m^3)			Accessible Porosity[e,h] (mℓ/kg of OPyC coating)	BAF_o[e,i]		
								Sink Float[f]		Calculated Bulk Density[g]				
		Mean	Standard Deviation			Mean	Standard Deviation	Mean	Standard Deviation			Mean	Standard Deviation	Faceting[c,d]
6542-27-0161-001	Yes	87	6.9	1.09	5.56	75	6.6	1.86[j]	0.006[j]	1.78[j]	23.3[k]	1.041[l]	0.085	8.58
-002	Yes	88	7.0	1.09	5.56	75	7.6	1.86[j]	0.006[j]	1.78[j]	23.3[k]	1.041[l]	0.085	8.58
6542-29-0261-001	Yes	94	6.9	1.13	4.59	76	9.8	1.96	0.042	1.89	19.5	1.081	0.009	8.97
-002	Yes	93	6.6	1.13	4.59	72	8.3	1.96	0.042	1.89	19.5	1.081	0.009	8.97
6542-39-0161-001	Yes	86	4.7	1.13	5.25	71	11.0	1.98	0.028	1.92	17.5	1.079	0.010	9.46
-002	Yes	86	6.6	1.13	5.25	74	9.4	1.98	0.028	1.92	17.5	1.079	0.010	9.46
6542-40-0161-001	Yes	91	5.8	1.10	5.15	73	7.0	1.74	0.011	1.67	25.0	1.042	0.003	6.84
-002	Yes	93	5.4	1.10	5.15	71	7.6	1.74	0.011	1.67	25.0	1.042	0.003	6.84
6542-40-0260-001	No	85	6.5	1.10	5.44	76	9.1	1.77	0.003	1.69	23.5	1.038	0.005	7.44
-002	No	88	6.1	1.10	5.44	77	7.8	1.77	0.003	1.69	23.5	1.038	0.005	7.44
6542-40-0261-001	Yes	89	6.0	1.10	5.44	78	7.2	1.77	0.003	1.70	22.5	1.038	0.005	7.44
-002	Yes	87	6.6	1.10	5.44	76	6.1	1.77	0.003	1.70	22.5	1.038	0.005	7.44
6542-41-0160-001	No	91	5.6	1.13	4.63	70	7.6	2.00	0.014	1.93	19.0	1.060	0.007	8.39
-002	No	88	6.3	1.13	4.63	68	7.4	2.00	0.014	1.93	19.0	1.060	0.007	8.39
6542-41-0161-001	Yes	92	6.3	1.13	4.63	69	6.4	2.02	0.035	1.93	22.5	1.081	0.012	8.39
-002	Yes	92	5.9	1.13	4.63	69	8.0	2.02	0.035	1.93	22.5	1.081	0.012	8.39

[a] Measured on capsule test samples by contact radiography.

[b] Measured by a mathematical calculation.

[c] Measured on as-coated parent batch.

[d] Measured using line-intercept technique on 200 particles on X-radiograph plates.
Equation used:

$$100 \times \frac{\sqrt{2}}{n} \sum_{i=1}^{n} \left(\frac{X_{1i} - X_{2i}}{X_{1i} + X_{2i}} \right)$$

where n = number of particles
X_1 = outer coating thickness on one side of particle
X_2 = outer coating thickness on other side of particle

[e] Measured on heat treated parent batches, except where noted, for the heat treated capsule test samples; otherwise the as-coated parent batches measured.

[f] >20 particles per batch measured by a liquid gradient technique.

[g] Calculated from equation $\frac{1}{\rho_B} = \frac{1}{\rho_{SF}} + K(AP)$, where ρ_B = bulk density, ρ_{SF} = sink float density, K = constant, and AP = accessible porosity.

[h] Measured on about 2 g of total coated particles using Hg porosimetry - the amount of Hg which intrudes into the coatings from 250 to 10,000 psi.

[i] Optical anisotropy measured with the Seibersdorf unit at GA using a 24-μm light spot at the center of the coating of 10 particles.

[j] Values for as-coated parent batch; data not available for heat-treated parent batch.

[k] Parent batch was heat treated for 60 minutes at 1650°C in He instead of 90 minutes in Ar for this QC measurement.

[l] 20 particles measured on batch heat treated at 1800°C for 60 minutes in He for this QC measurement.

TABLE 4-6
PROPERTIES OF TOTAL COATED BISO PARTICLES FOR HT-33 CAPSULE

Particle Batch Numbers				Total Diameter[a] (μm)		Particle Density[b] (Mg/m^3)		Density of Liquid Used to Separate Particles (Mg/m^3)	Th Content[c] (wt %)	Impurities[d] (ppm)		Fraction Defective in Coated Particles[c,f]	Exposed Th[c] (kg Th/kg Th)		Fission Gas Release[i]
	Parent Batch														
Capsule Sample	Data Retrieval 6542-	Manufacturer	Heat Treatment	Mean	Standard Deviation	Mean	Standard Deviation			Fe	Boron Equivalent[e]		Leach Test[g]	Hydrolysis Test[h]	
6542-27-0161-001	27-015	6291-53	Yes	823	23.0	3.45	0.018	3.45	56.8	28	1.27	0	3.7×10^{-6}	1.4×10^{-5}	3.4×10^{-6}
-002	27-015	6291-53	Yes	829	17.8	3.45	0.018	3.45	56.8	28	1.27	0	3.7×10^{-6}	1.4×10^{-5}	3.4×10^{-6}
6542-29-0261-001	29-025	6779-147	Yes	843	20.2	3.45	0.006	3.40	54.9	21	0.80	0	6.1×10^{-7}	5.9×10^{-5}	6.1×10^{-5}
-002	29-025	6779-147	Yes	833	17.3	3.45	0.006	3.40	54.9	21	0.80	0	6.1×10^{-7}	5.9×10^{-5}	6.1×10^{-5}
6542-39-0161-001	39-015	6779-151	Yes	821	19.9	3.61	0.022	3.56	58.9	25	0.85	0	4.5×10^{-7}	8.7×10^{-5}	6.2×10^{-6}
-002	39-015	6779-151	Yes	826	18.7	3.61	0.022	3.56	58.9	25	0.85	0	4.5×10^{-7}	8.7×10^{-5}	6.2×10^{-6}
6542-40-0161-001	40-015	6777-21	Yes	828	14.7	3.35	0.005	3.35	57.1	17	0.84	0	5.1×10^{-4}	7.6×10^{-6}	$<1.4 \times 10^{-6}$
-002	40-015	6777-21	Yes	827	21.7	3.35	0.005	3.35	57.1	17	0.84	0	5.1×10^{-4}	7.6×10^{-6}	$<1.4 \times 10^{-6}$
6542-40-0260-001	40-025	6777-23	No	829	20.0	3.36[j]	0.177[j]	3.35	57.0	19	0.77	0	2.2×10^{-5}	2.1×10^{-7}	3.6×10^{-6}
-002	40-025	6777-23	No	826	19.7	3.36[j]	0.177[j]	3.35	57.0	19	0.77	0	2.2×10^{-5}	2.1×10^{-7}	3.6×10^{-6}
6542-40-0261-001	40-025	6777-23	Yes	832	17.3	3.39	0.028	3.35	57.0	19	0.77	0	2.2×10^{-5}	2.1×10^{-7}	$<1.4 \times 10^{-6}$
-002	40-025	6777-23	Yes	828	17.0	3.39	0.028	3.35	57.0	19	0.77	0	2.2×10^{-5}	2.1×10^{-7}	$<1.4 \times 10^{-6}$
6542-41-0160-001	41-015	6777-5	No	827	19.7	3.51[j]	0.029[j]	3.45	56.0	24	0.87	0	1.5×10^{-5}	3.4×10^{-6}	4.2×10^{-5}
-002	41-015	6777-5	No	817	20.6	3.51[j]	0.029[j]	3.45	56.0	24	0.87	0	1.5×10^{-5}	3.4×10^{-6}	4.2×10^{-5}
6542-41-0161-001	41-015	6777-5	Yes	825	18.0	3.54	0.007	3.45	56.0	24	0.87	0	1.5×10^{-5}	3.4×10^{-6}	5.6×10^{-5}
-002	41-015	6777-5	Yes	823	18.1	3.54	0.007	3.45	56.0	24	0.87	0	1.5×10^{-5}	3.4×10^{-6}	5.6×10^{-5}

[a] Measured on capsule test samples using contact radiography.

[b] Density of 30 particles from density-separated fraction measured by liquid gradient technique; measured on separated samples after heat treatment of 1650°C for 90 minutes in vacuum except where noted.

[c] Calculated from parent batch densities and dimensions of density-separated fraction for the particle components and the kernel composition.

[d] Measured on as-coated parent batches.

[e] The following elements were measured by spectrographic analysis: Al, Be, Cd, Fe, Mo, P, Sn, V, B, Bi, Cr, Mg, Na, Pb, Sr, Zn, Ba, Ca, Cu, Mn, Ni, Si, and Tl.

[f] Measured on ≥2000 particles using contact radiography.

[g] 10-g samples were leached for 24 hours except batch 6542-27-015 (5 hours) in acid.

[h] 25-g samples heated in vacuum at 1800°C for 1 hour before hydrolysis; no correction factor has been used.

[i] Release rate/birth rate for Kr-85m at 1100°C (in linear accelerator); 20-g samples measured on heat-treated parent batches, except for 6542-27-0161-001 and -002, for the heat-treated capsule test samples; otherwise, the values of the as-coated batches are reported.

[j] Measured after heat treated at 1400°C for 1 hour in vacuum.

TABLE 4-7
HTGR SPECIFICATIONS OF KERNELS[a]

Attribute	Specification[b] Value
Diameter	
Mean (μm)	480 - 520
Range[c] (μm)	400 - 600
Fraction in critical region (>615 μm)	≤0.01
Shape (percent of kernels with a ratio of maximum diameter/ minimum diameter ≥1.2)	≤10
Density (Mg/m^3)	≥9.50
Chemical Composition (ppm-wt)	
Fe	≤100
Cr	≤100
Ni	≤100
Na	(d)
Ca	(d)
Total impurities	≤5000

[a] No kernel properties were out-of-specification.
[b] From Ref. 4-3.
[c] 95% of kernels shall be in indicated range.
[d] To be determined.

TABLE 4-8
HTGR SPECIFICATIONS AND OUT-OF-SPECIFICATION PROPERTIES OF BISO COATED PARTICLE BATCHES FOR HT-33 CAPSULE

Attribute	Specification Value	Out-of-Specification Items[b]					
		6542-27-015	6542-29-025	6542-39-015	6542-40-015	6542-40-025	6542-41-015
Buffer							
Thickness							
Mean (μm)	80 - 110						
Fraction in critical region (≤52 μm)	≤0.01						
Density (Mg/m^3)	0.90 - 1.20						
Diluent and carrier gas	Ar						
Coating gas	C_2H_2						
OPyC							
Thickness							
Mean (μm)	70 - 90						
Fraction in critical region (≤46 μm)	≤0.01						
Density[c]							
Mean (Mg/m^3)	1.80 - 1.95		1.96		1.74	1.77	2.00
Fraction in critical region <1.75 Mg/m^3	<0.02				(d)	(d)	
≥2.00 Mg/m^3	≤0.02						(d)
Coating rate (μm/min)							
Minimum	≥2.5						
Maximum	≤8.0						
BAF_o	(e)						
Porosity (%)	(e)						
Faceting (%)	(e)						
Diluent and carrier gas	Ar or N_2				H_2	H_2	
Coating gas	C_2H_2/C_3H_6						
Defective Particles							
Excessive fuel dispersion plus missing or incomplete buffer coating	$\leq 1 \times 10^{-3}$ (total for both)						
Missing or incomplete outer isotropic coating	$\leq 1 \times 10^{-3}$						
Boron Equivalent							
Burnable boron equivalent (ppm by weight)	≤5.0						
Nonburnable boron (ppm by weight)	≤1.0						

[a] From Ref. 4-3.
[b] Measured on parent batches.
[c] Measured by liquid gradient technique.
[d] Does not meet the specification.
[e] Acceptance criteria to be determined.

TABLE 4-9
COMPARISON OF AS-COATED AND HEAT-TREATED PROPERTIES OF THE PARTICLE BATCHES FOR HT-33 CAPSULE[a,b]

Parent Batch Number[c]	Buffer Thickness (μm)		OPyC Coating										Fission Gas Release[d]		Total Particle Density[e] (Mg/m³)		Heat-Treatment Condition of HT-33 Sample	
			Thickness (μm)		Density (Mg/m³)				Accessible Porosity (mℓ/kg coatings)		BAF_o							
					Liquid Gradient		Bulk											
	As-Coated	1650°C	As-Coated	1650°C	As-Coated	1650°C	As-Coated	1650°C	As-Coated	1650°C	As-Coated	1650°C	As-Coated	1650°C	As-Coated	1650°C	As-Coated	1650°C
6542-27-015	84	(f)	81	(f)	1.86	(f)	1.78	(f)	23.0	23.3[g]	1.032	1.041[h]	3.4×10^{-6}	(f)	3.49	3.46		X
6542-29-025	96	93	74	72	1.96	1.96	1.89	1.89	18.5	19.5	1.060	1.081	2.6×10^{-5}	6.1×10^{-5}	3.43	3.45		X
6542-39-015	89	87	73	72	1.94	1.98	1.88	1.92	17.3	17.5	1.060	1.079	1.9×10^{-5}	6.2×10^{-6}	3.63	3.61		X
6542-40-015	95	(f)	73	(f)	1.73	1.74	1.67	1.67	22.7	25.0	1.044	1.042	4.1×10^{-6}	$<1.4 \times 10^{-6}$	3.35	3.35		X
6542-40-025	89	(f)	79	(f)	1.76	1.77	1.69	1.70	23.5	22.5	1.038	1.038	3.6×10^{-6}	$<1.4 \times 10^{-6}$	3.36	3.39	X	X
6542-41-015	95	91	72	70	2.00	2.02	1.93	1.93	19.0	22.5	1.060	1.081	4.2×10^{-5}	5.6×10^{-5}	3.51	3.54	X	X

[a] Each batch heat treated at 1650°C for 90 minutes in Ar except where noted.

[b] Properties measured on the parent batches.

[c] The capsule samples have the number 6 instead of a 5 for the ninth number; i.e., batch 6542-27-015 is the parent batch for sample 6542-27-0161-001.

[d] Release rate/birth rate at 1100°C for Kr-85m.

[e] Measured by liquid gradient technique.

[f] Not determined.

[g] Batch heat treated at 1650°C for 60 minutes in He for this QC measurement.

[h] Batch heat treated at 1800°C for 60 minutes in He for this QC measurement.

TABLE 4-10
COMPARISON OF HT-33 BISO BATCHES BEFORE AND AFTER SCREENING AND DENSITY SEPARATION[a]

Attribute	6542-27-015[b]		6542-29-025[b]		6542-39-015[b]		6542-40-015[b]		6542-40-025[b]		6542-41-015[b]	
	Parent	Daughter	Parent	Daughter	Parent	Daughter	Parent	Daughter	Parent	Daughter	Parent	Daughter
Dimensions[c] (μm)												
Kernel diameter												
Mean	512	(d)	505	511	505	515	508	502	502	501	506	509
Standard deviation	9.69	(d)	10.71	11.40	11.43	12.69	13.17	10.32	11.59	9.86	11.56	12.29
Buffer thickness												
Mean	84	(d)	96	88	89	74	95	92	89	87	95	82
Standard deviation	11.64	(d)	13.12	8.99	10.92	9.66	14.05	7.09	13.71	6.79	11.81	9.85
OPyC thickness												
Mean	81	(d)	74	82	73	76	73	75	79	78	72	79
Standard deviation	7.89	(d)	8.51	9.79	9.95	10.05	8.22	6.82	8.30	7.06	8.10	8.93
Coated particle diameter												
Mean	836	(d)	843	844	828	812	846	835	839	832	839	820
Standard deviation	41.12	(d)	33.61	24.27	32.04	32.34	37.07	17.79	33.29	19.09	33.02	30.18
Total particle density[e] (Mg/m^3)	3.47	3.49	3.42	3.43	3.57	3.63	3.33	3.35	3.33	3.36	3.43	3.51

[a] The properties were measured on samples which were not heat treated except where noted.

[b] Parent particle batch number. The capsule samples have the number 6 instead of a 5 for the ninth number; i.e. batch 6542-27-015 is the parent batch for sample 6542-27-0161-001.

[c] Measurements taken on 200 total coated particles or x-radiograph plate. Daughter batch measurements taken after screening.

[d] Not determined.

[e] The density was measured with an air pycnometer for the parent batches and with a liquid density gradient column for the daughter batches which were given the standard heat treatment (1400°C) for density-separated samples.

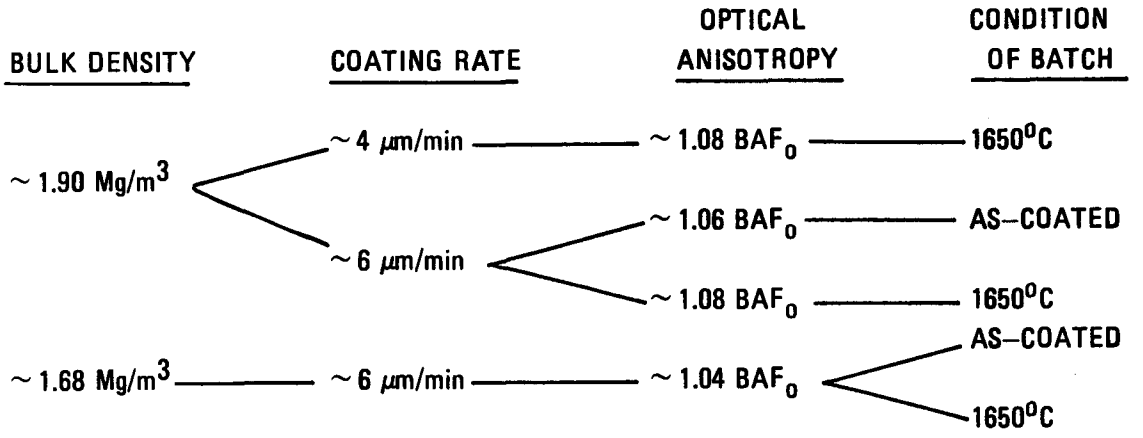

Fig. 4-1. Test matrix of primary OPyC coating variables of ThO_2 BISO batches made in the large coater for capsule HT-33

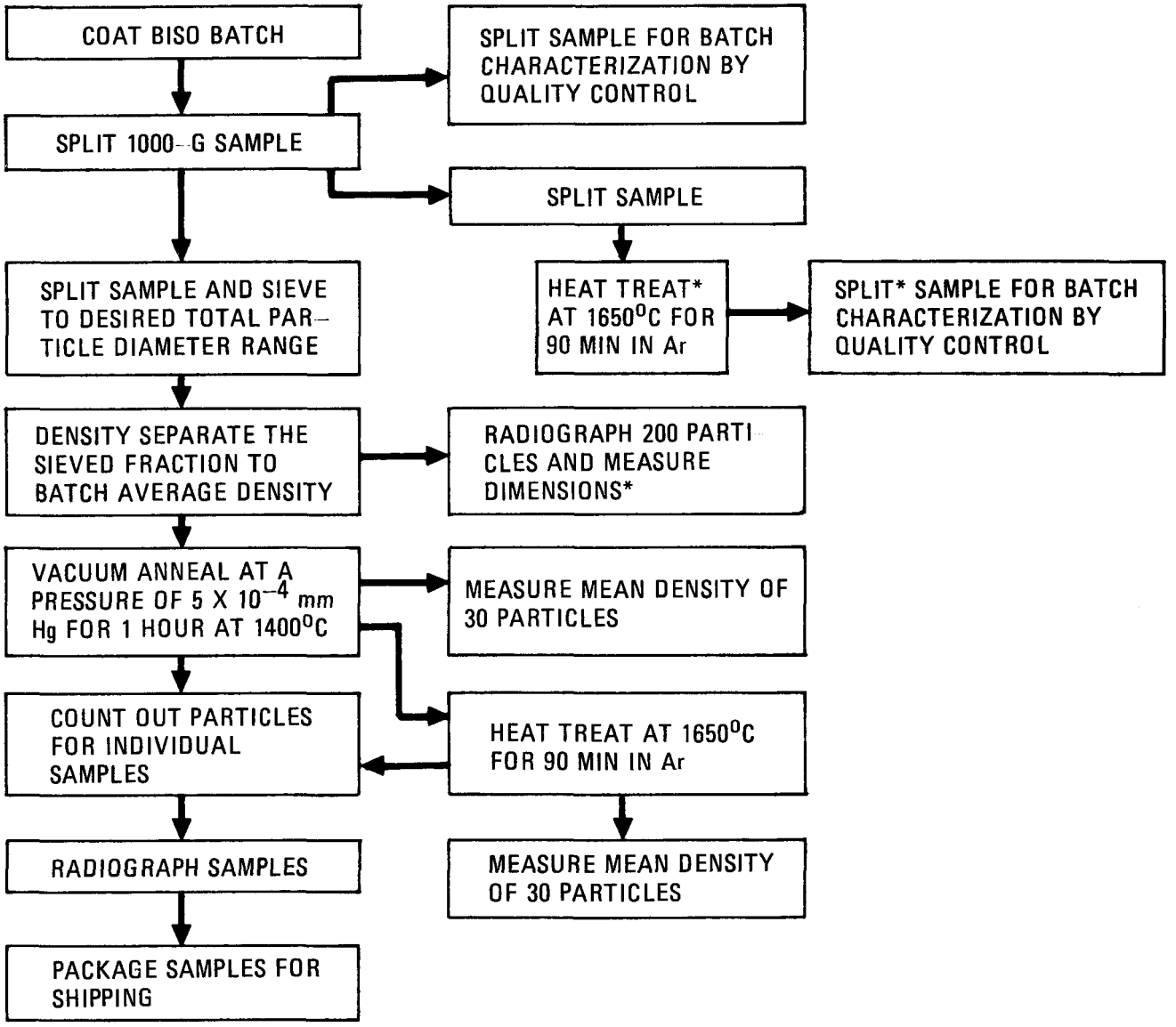

Fig. 4-2. Steps involved in obtaining the BISO coated ThO_2 particle samples for irradiation capsule HT-33. The operations marked with an asterik were not performed on parent batch 6542-27-015.

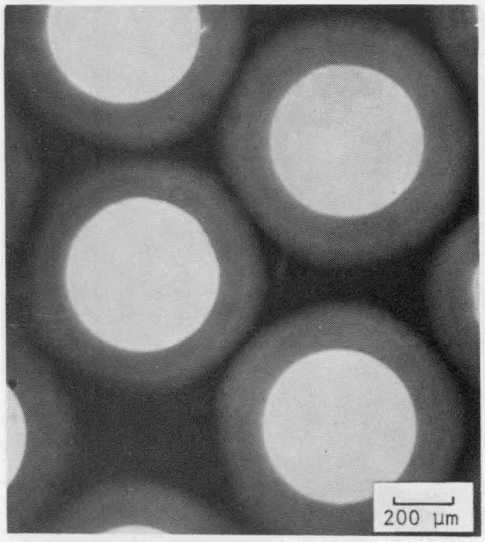

LA109-2 (a)

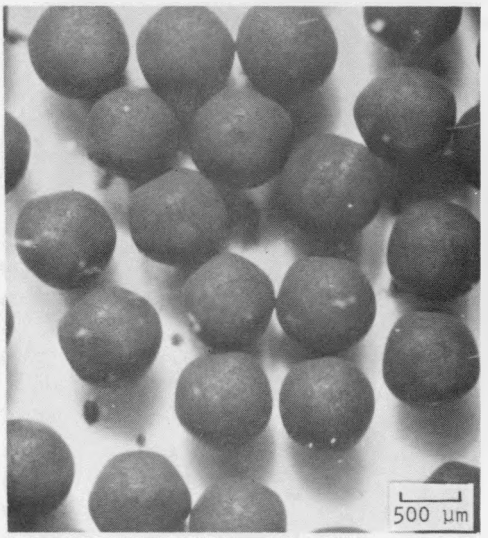

SP74012-1 (b)

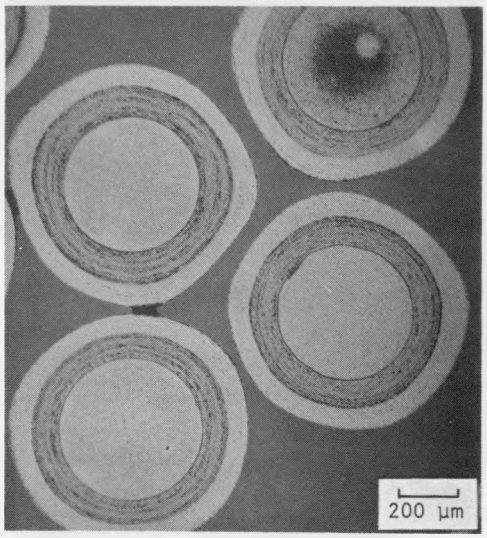

MP74031-2 (c)

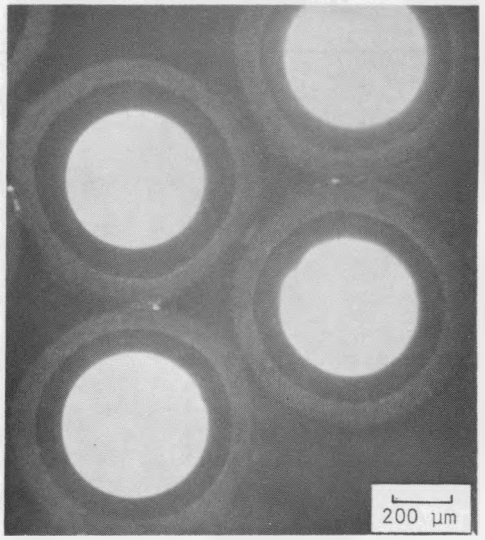

MP74031-1 (d)

Fig. 4-3. Representative photomicrographs of BISO coated ThO_2 particles from batch 6542-27-015 for capsule HT-33: (a) radiograph, (b) stereo view, (c) bright field, (d) polarized light

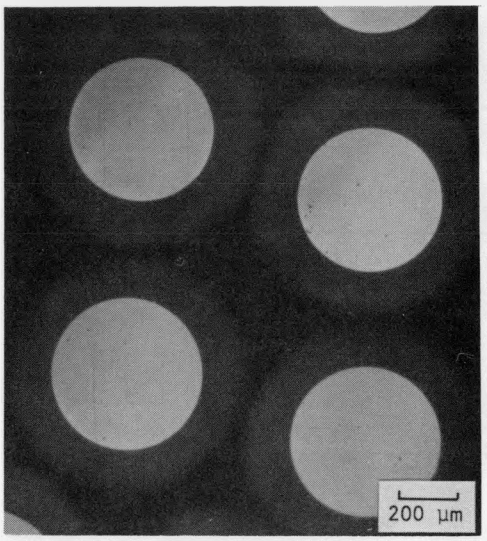

LB378-2 (a)

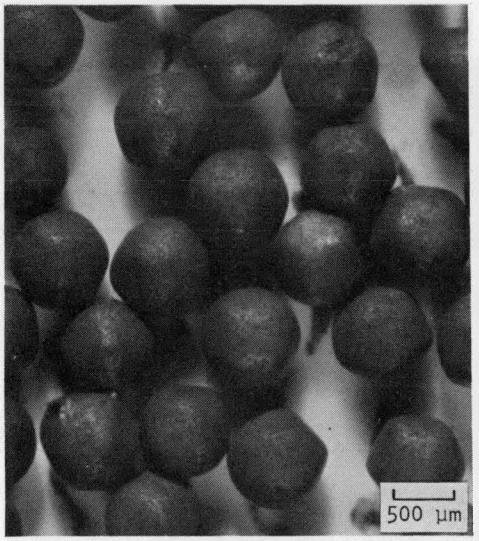

SP76002-1 (b)

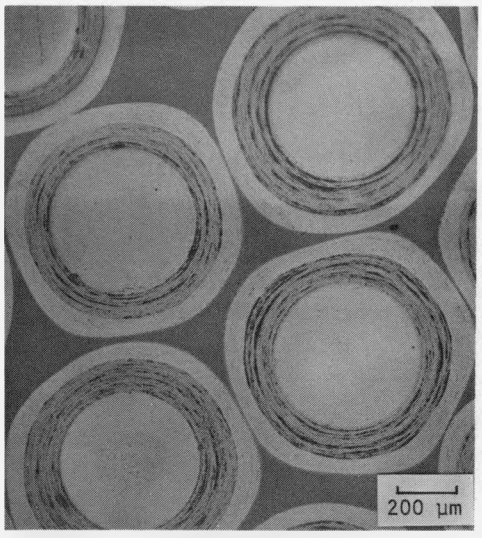

MP76009-1 (c)

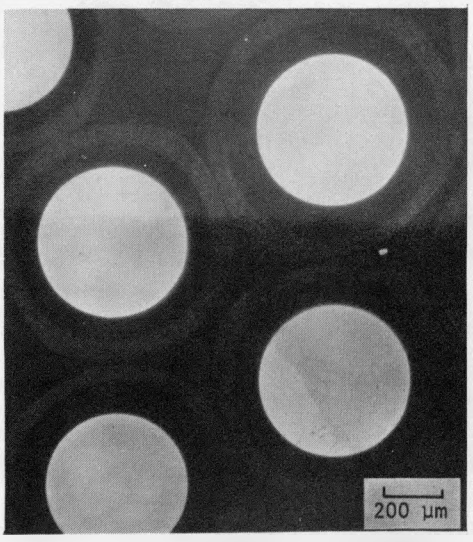

MP76009-2 (d)

Fig. 4-4. Representative photomicrographs of BISO coated ThO_2 particles from batch 6542-29-025 for capsule HT-33: (a) radiograph, (b) stereo view, (c) bright field, (d) polarized light

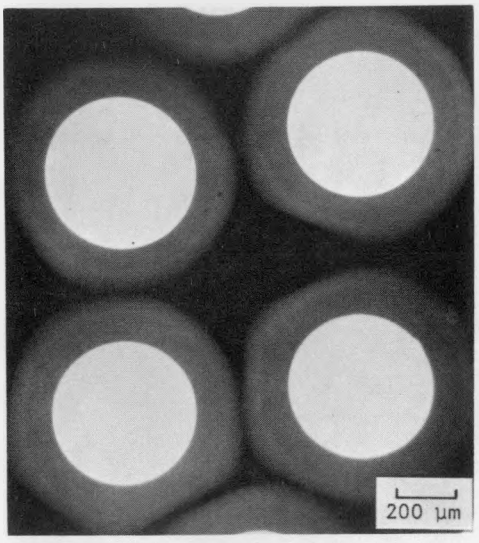

LB380-2 (a)

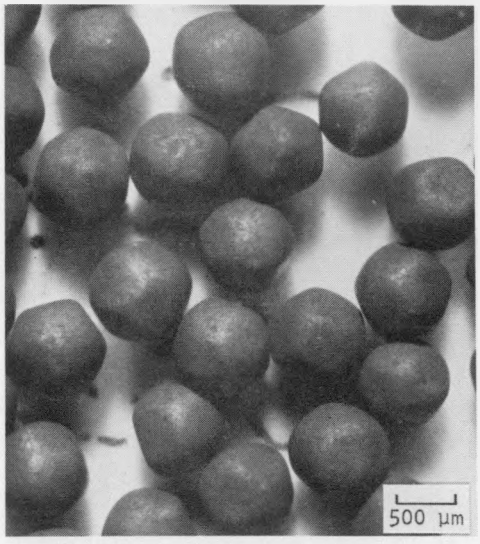

SP76004-1 (b)

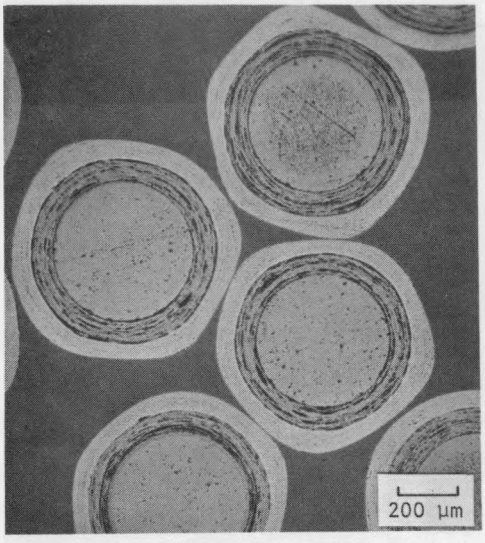

MP76011-6 (c)

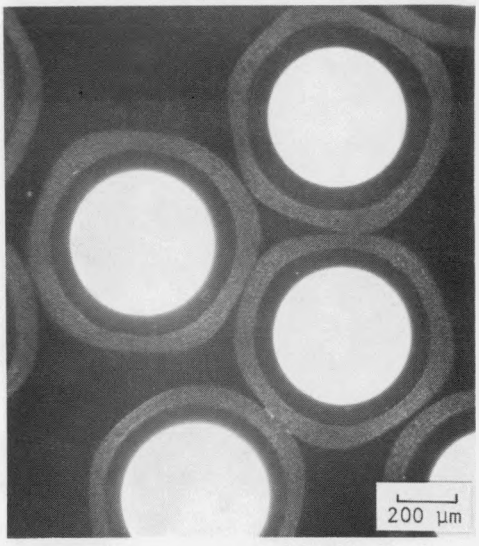

MP76011-7 (d)

Fig. 4-5. Representative photomicrographs of BISO coated ThO_2 particles from batch 6542-39-015 for capsule HT-33: (a) radiograph, (b) stereo view, (c) bright field, (d) polarized light

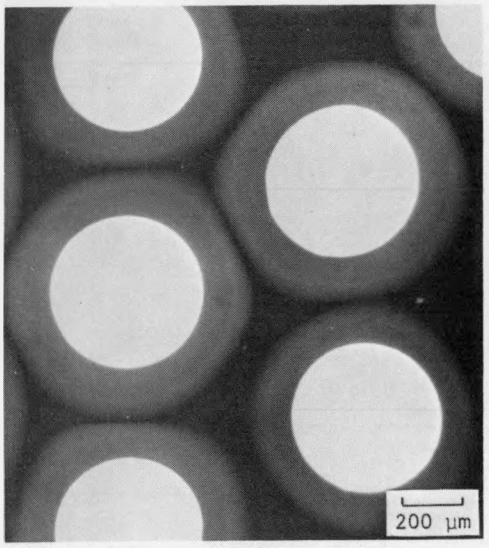

LB400-2 (a)

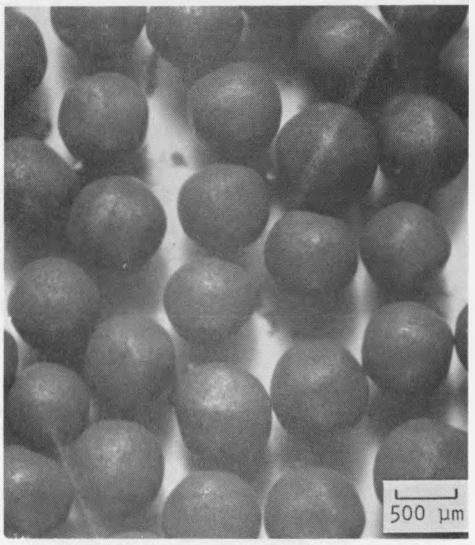

SP76024-1 (b)

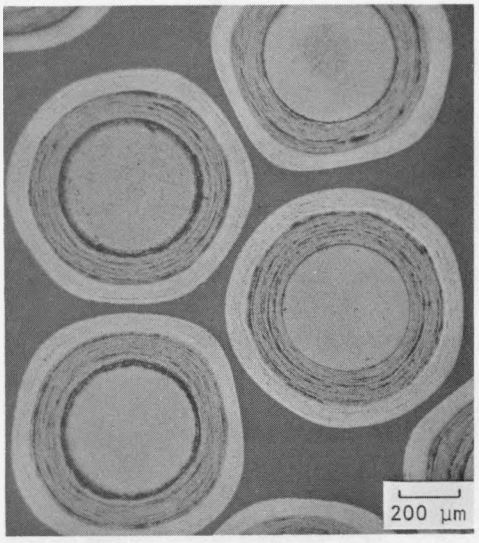

MP76031-1 (c)

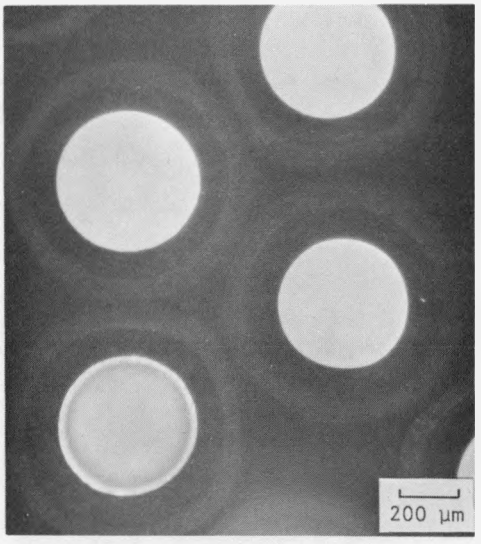

MP76031-2 (d)

Fig. 4-6. Representative photomicrographs of BISO coated ThO_2 particles from batch 6542-40-015 for capsule HT-33: (a) radiograph, (b) stereo view, (c) bright field, (d) polarized light

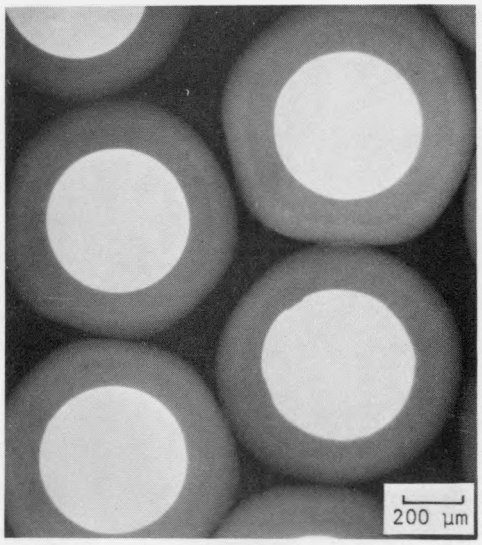

LB417-2 (a)

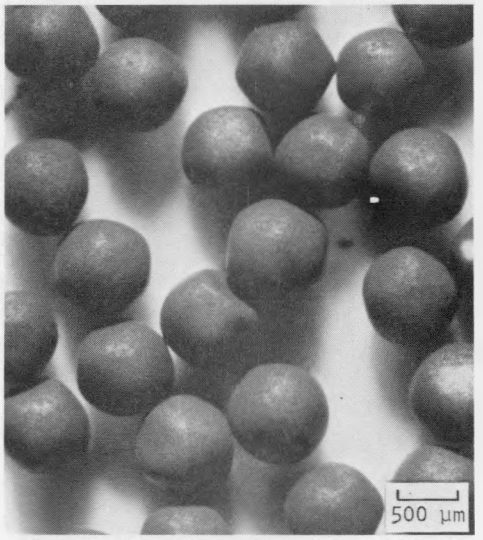

SP76025 (b)

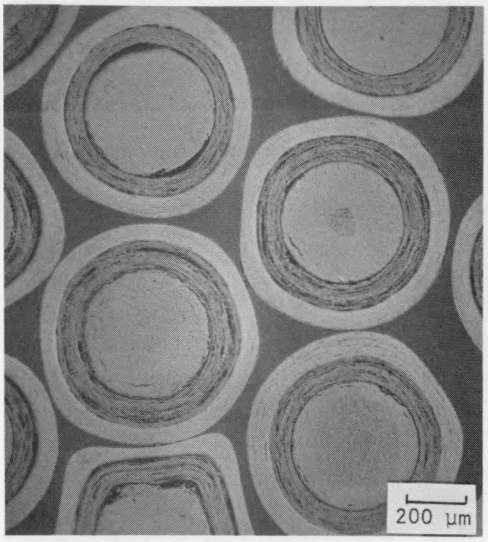

MP76032-1 (c)

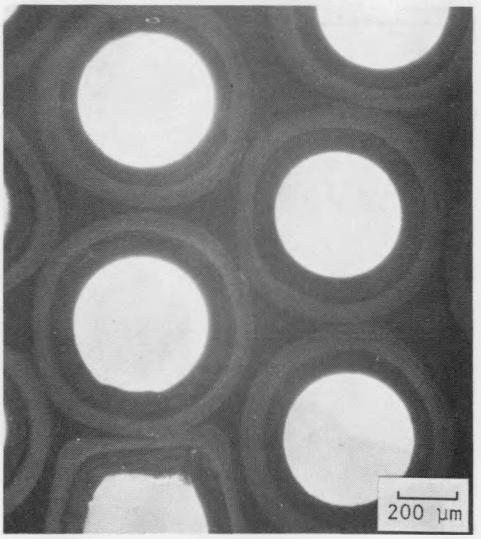

MP76032-2 (d)

Fig. 4-7. Representative photomicrographs of BISO coated ThO_2 particles from batch 6542-40-025 for capsule HT-33: (a) radiograph, (b) stereo view, (c) bright field, (d) polarized light

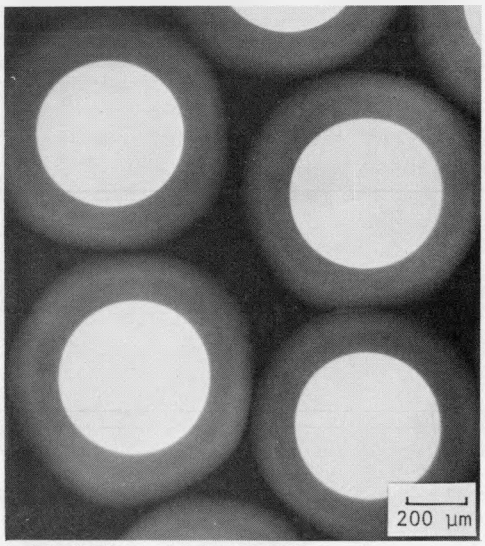

LB383-2 (a)

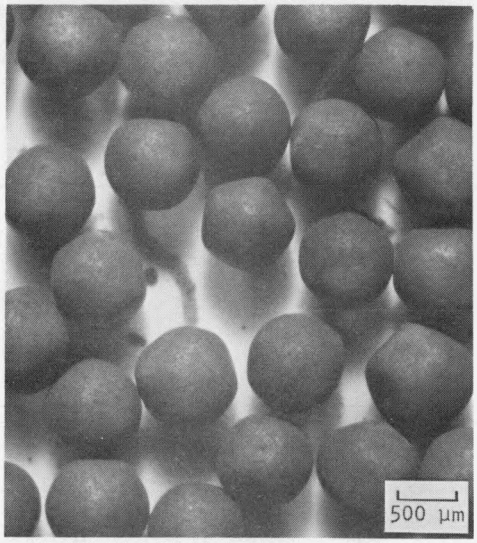

SP76005-1 (b)

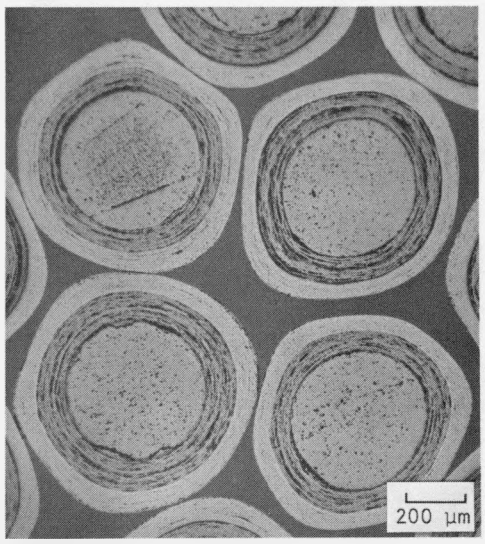

MP76012-6 (c)

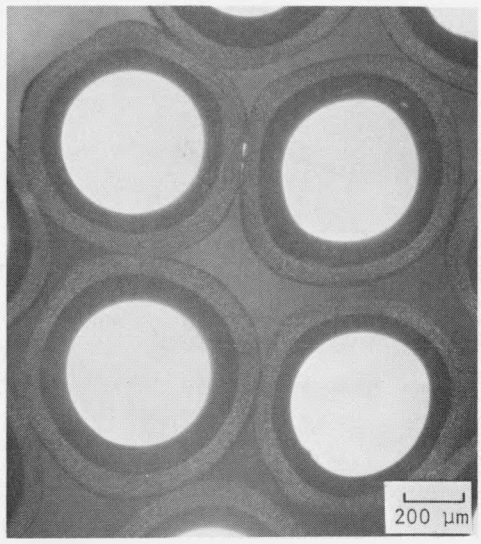

MP76012-7 (d)

Fig. 4-8. Representative photomicrographs of BISO coated ThO_2 particles from batch 6542-41-015 for capsule HT-33: (a) radiograph, (b) stereo view, (c) bright field, (d) polarized light

5. POSTIRRADIATION EXAMINATION

Postirradiation examination of the TRISO and BISO coated ThO_2 particles is scheduled to include the following:

1. Visual observation to determine and categorize OPyC and SiC failure fractions.

2. Radiography and metallography.

3. Characterization of burnup.

In addition, a limited number of irradiated particles will serve as historical samples. These particles will be designated for future use in optical anisotropy measurements defining structural variations in the OPyC during irradiation and/or thermal stability tests defining amoeba migration and rare earth fission product interactions in the particle.

6. ACKNOWLEDGMENTS

The authors would like to acknowledge P. R. Macy, M. S. Cronin, and W. R. Ziegler for the preparation of the HT-31 and HT-33 capsule samples and the reduction of the QC data. The assistance of all personnel who fabricated the coated fuel particles is greatly appreciated. In particular, the efforts of C. C. Adams, who was in charge of the coating operations, is gratefully acknowledged.